Copy_________

06515-2-T

THE UNIVERSITY OF MICHIGAN

COLLEGE OF ENGINEERING
DEPARTMENT OF ELECTRICAL ENGINEERING
Radiation Laboratory

STUDY OF PROBLEM AREAS IN OPTICAL COMMUNICATIONS

Interim Report No. 2

1 July through 30 September 1964

Contract AF 33(615)-1021

G. Hok, M. L. Barasch, P. Lambropoulos and E. K. Miller

31 October 1964

6515-2-T = RL-2138

Contract With:

Air Force Avionics Laboratory, AVWC
Research and Technology Division
Wright-Patterson Air Force Base, Ohio
45433

Administered through:

OFFICE OF RESEARCH ADMINISTRATION • ANN ARBOR

TABLE OF CONTENTS

ABSTRACT

In the problem area of atmospheric absorption and scattering of electromagnetic waves in the visible and infrared ranges, the strong and weak absorption bands associated with the various regular constituents of the atmosphere have been evaluated from available data reported in the literature. Absorption coefficients and abundance figures are tabulated in the report. The effects of rain, clouds, fog, and haze have also been studied.

The communication theory of optical channels has been the subject of further investigation. A receiver incorporating a laser preamplifier has been analyzed and compared with a receiver that simply counts the number of photons received in each sampling interval. A more specific discussion is presented for the case of a binary channel.

Optical filters for elimination of interfering signals as well as background noise radiation outside the channel frequency band constitute the third problem area. During the reporting period a detailed analysis of the properties of a Wernicke prismatic filter has been undertaken. The conclusions regarding the prospect of achieving satisfactory performance for the above purpose are negative. A corresponding investigation has been made of a polarization interference filter. As far as theoretical limitations are concerned, the conclusions are more favorable, although the state-of-the-art does not appear ready for a satisfactory practical solution for this application.

INTRODUCTION

The introduction to the first Interim Report[1+] gave a brief survey and discussion of the problem areas with which this project is concerned and of the objectives toward which it is directed. This material will not be repeated here; we shall only give, as a guide to the main body of this second Interim Report, a brief outline of the subject matter that has been given major attention during the period July through September 1964.

The work in the problem area of atmospheric absorption and scattering during the period has included a survey of strong and weak absorption bands associated with the various constituents of the atmosphere, as well as a collection of pertinent data from the available literature regarding their absorption coefficient and abundance. The effects of haze, fog, clouds, and rain have also been studied.

In the communication-theoretical problem area further critical attention has been given to the theoretical limits for the rate of transmission of information by means of photon beams. A receiver incorporating a laser preamplifier has been analyzed and compared with a receiver that simply counts the number of photons received in a sampling interval. A more specific discussion is presented for the case of a binary channel.

In the third problem area, optical bandpass filters, two different filter principles have been investigated. The transmissivity and bandwidth of a Wernicke prismatic filter have been derived; the conclusions reached are that this principle does not appear promising for the input end of a photon-counter receiver. Corresponding calculations for a polarization interference filter reveal fewer theoretical limitations, even though, at the present, state-of-the-art considerations of bulk, weight, absorption loss, etc., are very unfavorable.

[+] Superscript numbers in this report refer to Reference Numbers - see Bibliography and the end of this report.

I. First Problem Area: Optical Communication Under Adverse Meteorological Conditions

1.1 Attenuation by Normal Constituents of the Atmosphere

1.1.1 Introduction

Attenuation by absorption may be described in terms of an absorption cross section γ, with the fractional transmission T_S over the path s given by

$$\ln T_S = - \sum_i \int_s \gamma_i(\vec{r}) n_i(\vec{r}) dl \quad , \qquad (1.1)$$

in which n_i is the abundance of the ith molecular species, and the summation extends over all species along the propagation paths.

This mechanism of attenuation is so strongly wavelength-dependent that avoiding spectral regions in which strong absorption is manifest would be wise. As will be found, there are, nevertheless, scattered weak absorption regions which would be difficult to avoid. To facilitate the evaluation of the practical significance of molecular avoidance, it will be necessary to present tables of values of γ and n for important species corresponding to both intrinsically strong and weak absorption bands.

Attenuation by scattering and broad-band absorption such as by dielectric loss, both of which may be present in fog, haze, rain, etc., will be treated in subsequent chapters.

1.1.2 Strong Absorption Bands

The strong absorption bands are listed in Table I below, and the corresponding abundance at sea level appear in Table III. Table I is based on Ref. 2 .

TABLE I: ABSORPTION BANDS OF SIGNIFICANT INTRINSIC STRENGTH

Band Center Wave Nr. cm^{-1}	Approximate Wavelength microns	Species	Absorption Cross Section cm^{-1} per cm NTP
3756	2.6	H_2O vapor	180
1597	6.3	H_2O vapor	300
5331	1.9	H_2O vapor	30
7250	1.4	H_2O vapor	20
667	15.0	CO_2	173
2349	4.3	CO_2	2480
3613	2.8	CO_2	28
3714	2.7	CO_2	25
1167	8.5	N_2O	8.5
1285	7.8	N_2O	245
2224	4.5	N_2O	1033
1306	7.7	N_2O	150
3019	3.3	N_2O	300
6005	1.7	N_2O	1

1.1.3 Weak Absorption Bands

This section presents data on bands which would be difficult to avoid, so that in contrast to the strong ones at which the atmosphere may simply be taken as opaque, it is of interest to be able to compute the absorption associated with these bands. Strengths of some weak bands appear in Table II. (Ref. 2).

TABLE II: SOME WEAK ABSORPTION BANDS

Band Center Wave Nr. cm^{-1}	Wavelength microns	Constituent	Absorption Coefficient cm^{-1} per cm NTP
2130	4.5	CO_2	0.0037
2093	4.6	CO_2	0.007
1933	5.2	CO_2	0.011
6228	1.6	CO_2	0.0077
4260	2.3	CO	1.80
1868	5.1	NO_2	0.40
6005	1.5	CH_4	0.96

In addition to these, water vapor exhibits a number of weak bands at diverse wavelengths. In the absence of reliable information on the abundance of water vapor (which is in any case highly variable), it does not appear useful to list these in Table IV. Abundances of other constituents have been cited in Refs. 3 and 4. They are presented both for the sea-level atmosphere (that table would then pertain to low-altitude situations) and the total atmosphere (which is important for communications with an extra-atmospheric vehicle).

As an indication that even weak bands at sea level can be significant, one may compute the transmission over 1 Km in the 1933 cm^{-1} band of CO_2 at sea level:

$$\ln T_{1Km} = -0.011 \times 32 = -0.352$$

$$T \cong 0.7 \quad .$$

Thus, there is non-negligible attenuation for even this illustrative calculation. It might be possible to communicate in spite of this loss. However, if transmission through the entire atmospheric thickness were required, one would predict a greater attenuation:

$$\ln T_{ATM} = -0.011 \times 320 = -3.52, \quad \text{and } T \cong 0.3 \quad .$$

TABLE III: SEA LEVEL ABUNDANCES

Constituent	Abundance at Sea Level Atom-cm per Km Path
CO_2	32.0
N_2O	0.027
CH_4	0.24
CO	0.11

TABLE IV: SOME TOTAL ABUNDANCES

Constituent	Total Atmospheric Abundance (atom-cm)
CO_2	320.0
CH_4	1.2
N_2O	0.4
CO	0.06 - 0.15
H_2O	10^3 - 10^4

1.1.4 Additional Considerations for Refining Absorption Calculations

Questions dealing with line shape (distribution of intensity within a single band) have been ignored in this chapter. One place they might arise is in the interpretation of the 'band-averaged' intensities cited by Ref. 1, which have here been taken as representative for frequencies within the band. Another point to which they pertain is the determination of the proper statistical procedure for obtaining the intensity in the wings of overlapping bands. In our opinion, it is justified to defer study of these questions while performing preliminary calculations; we have accordingly done so.

Intensity will vary with altitude (through temperature and pressure) as the line width varies, and so will the population of the originating levels of the band. This refinement could be considered at some later time.

Not merely ranges of variation of abundances of atmospheric constituents, but probabilities of each value are significant as an indication of whether extreme values are to be expected.

Absorption by water vapor, which exhibits very many infrared bands, both strong and weak, has not been computed. More precise data on the abundance of water should be obtained before such calculations can be performed.

1.2 Attenuation by Meteorological Conditions

1.2.1 Introduction

In the first chapter of this report, attenuation associated with absorption bands of atmospheric gases was considered. The present chapter is devoted to extinction resulting mainly from scattering by rain, clouds, haze, fog and such phenomena. Scattering by gas molecules and by the haze component associated with clear standard atmosphere are also investigated here.

In general, it is found that satisfactory definitions of the weather phenomena, with precisely specified size distributions of the suspended matter, do not exist. As a result, it is difficult to select cases in which calculations apply to situations identical to those for which experiments have been performed so that comparison of theory and experiment has not proved fruitful here. It is also difficult to establish whether the situations considered separately by various investigators are in any respects typical. For these reasons, a compilation of data without exhaustive correlation or precise conclusion is the only procedure justified by the state of research in this area. Nevertheless, the few conclusions apparently permissible will appear in the balance of this chapter.

1.2.2 Rain

In a heavy rainstorm, a typical raindrop[4] may have a radius of 1 mm, and the abundance of such drops be only $10^{-3}/cm^3$. For the frequencies of interest, these drops are large enough that the approximate value of the total scattering cross section σ is given by equation (1.2) where r is the radius,

$$\sigma = 2\pi\ r^2 \ . \tag{1.2}$$

It follows that the corresponding extinction coefficient α, is given by

$$\alpha = 2N\ \pi\ r^2 \tag{1.3}$$

or

2π per Km ,

where N is the abundance. This equation predicts that the frequencies of interest, in traversing 1 Km through a heavy rainstorm, would exhibit a transmissivity of approximately $\exp(-2\pi)$, or, in other words, be considerably attenuated. It is known that absorption by the water droplets may be neglected in comparison with scattering losses[6], and it has, therefore, not been treated here. A calculation of α incorporating a more precise formulation is in process, and is expected to yield a somewhat lower value.

1.2.3 Clouds

These are mixtures of water droplets, ice crystals, and some water vapor.

There is much variation between clouds, and indeed in the course of evolution of any individual cloud. For this reason, it is felt that it is of more value to cite here the results of experiments performed under a wide variety of cloud -cover conditions than to refer to calculations such as those of Deirmendjan[7].

The data presented in reference 7 were obtained in a spectral region lying between 0.1μ and 15 μ for transmission through a large variety of mixtures of cirrus, cumulus, and nimbus cloud covers.

Near 0.5 μ, the transmissivities varied between roughly 20 per cent and 95 per cent.

Above 10 μ, they ranged from 30 per cent up.

The conclusion to be drawn here is that clouds may present significant attenuation, but not total opacity.

1.2.4 Hazes, Fogs

The situation with regard to comparison of theory and experiment, or applicability of experimental results as "typical", is as bad here as for clouds. Therefore, it must suffice here to cite a few numbers obtained from the literature[9,10]. A number of fogs in the Chesapeake Bay region yielded attenuation coefficients (in the spectral region 0.30 μ - 3 μ) which were usually between 0.02 km^{-1} and 2 km^{-1}. This wide a variation does not permit drawing a practical conclusion. Another series of measurements in Chicago on days of fog and generally poor weather, during the course of formation of fog, for the band 1 - 10 μ showed the optical density σL to be between 0.1 and 1.0 typically, where the path L was 200 yards. In other words, the scattering attenuation coefficient σ varied between 1/2000 yard or roughly $0.5 Km^{-1}$ and roughly $5 Km^{-1}$. Again, no conclusion is possible. In both references, the curves reported do exhibit better transmission for the large wavelength end of the band. The latter measurements do not exceed attenuations of $0.4 Km^{-1}$ for $\lambda > 2\ \mu$, nor do the former. It appears then, that this end of the band is preferable for transmissions through fog and haze.

Reference 7 contains calculations based on integration of the exact Mie solution over assumed droplet size distributions for fogs, incorporating the frequency dependence of the dielctric constant. The computed attenuation coefficients decrease from roughly $1 Km^{-1}$ near .5 μ to slightly smaller values near 10 μ, in agreement with the trend but not the precise values obtained by experiment. Any conclusion which is to serve as a foundation for important decision must await further experimental investigations which may clarify the situation.

1.2.5 Clear - Atmosphere Haze

The model of a Clear Standard Atmosphere contains a haze component, as discussed by Reference 10. Attenuation of infrared radiation by a given aerosol distribution is computed. The attenuation coefficient for wavelengths below 0.5 μ was computed to be 0.20 Km^{-1} at sea level, while for the band 0.5 μ - 5 μ, an approximately linear decrease to a value of 0.05 Km^{-1} was predicted.

1.2.6 Rayleigh Molecular Scattering

Yet another mechanism attenuating infrared radiation even in clear weather is the scattering by molecules of the atmospheric gases, which, since the molecules are much smaller than the wavelength, is referred to as Rayleigh scattering. A calculation of this effect employing molecular abundances based on the U.S. Standard Atmosphere appears in Ref. 10. The attenuation at 0.55 μ and sea level is roughly $10^{-2}Km^{-1}$, decreasing rapidly with altitude as abundance falls. For larger wavelengths, the attenuation is orders of magnitude smaller.

II. Second Problem Area: Information Efficiency and Choice of Detection System

2.1. Some Comments on Quantum Communication Theory

The relations between the classical communication theory and its extensions to frequencies and power levels where quantum phenomena governs the behavior of physical systems offer a number of difficulties for the intuitive acceptance and the synthesis of a consistent logical structure.

Consider the maximum wave entropy or 'informational wave capacity' introduced by Gordon[12] and reviewed in Section 2.1 of the first Interim Report on this contract[1]. Adopting a system of harmonic oscillators as a model of a propagating channel with given average signalling power, the equation (2.2) in Ref. 1, or in terms of a single pair of samples and the expected value $\bar{m}$ of the number of photons per sample pair:

$$C_s = \log(1+\bar{m}) + \bar{m}\log(1+\frac{1}{\bar{m}}) \tag{2.1}$$

The first term has been compared to Shannon's entropy of a Gaussian signal in Gaussian noise

$$C_{cl} = \log(1+\frac{S}{N}) \tag{2.2}$$

per sample pair. With the 'quantum uncertainty' or 'quantum noise power' $N = hf \cdot \Delta f$ and S, taken to be the average signal power $S = \bar{m} \cdot hf \cdot \Delta f$ there appears to be a striking analogy.

It should be noted, however, that in the classical limit $\bar{m} \gg 1$ the second term does not approach zero but rather a limit value equal to log e.

In the opposite extreme $\bar{m} \ll 1$, the approximate values of the two terms are

$$C_s \cong \bar{m} + \bar{m}\,(\log\frac{1}{\bar{m}} + \bar{m}). \tag{2.3}$$

The second term predominates in this case.

The fact that the entropy breaks down into two terms that behave very differently in the limits can be shown to be a consequence of the exponential form of the maximum-entropy distribution.

As shown in the above references, the probability of there being exactly m photons stored in a harmonic oscillator in equilibrium at temperature $T^{o}K$ may be written

$$p(m) = C \cdot \exp\left[-m \cdot \frac{hf}{KT}\right] = \frac{1}{1+\bar{m}}\left[\frac{\bar{m}}{1+\bar{m}}\right]^{m} . \tag{2.4}$$

This geometric progression of probabilities can be simply illustrated by a lopsided 'tree' composed of an infinite number of subsequent identical random binary choices (Fig. 2-1). The two probabilities in the diagram are

$$p = p(0) = \frac{1}{1+\bar{m}} \tag{2.5}$$

$$q = 1 - p(0) = \frac{\bar{m}}{1+\bar{m}} \tag{2.6}$$

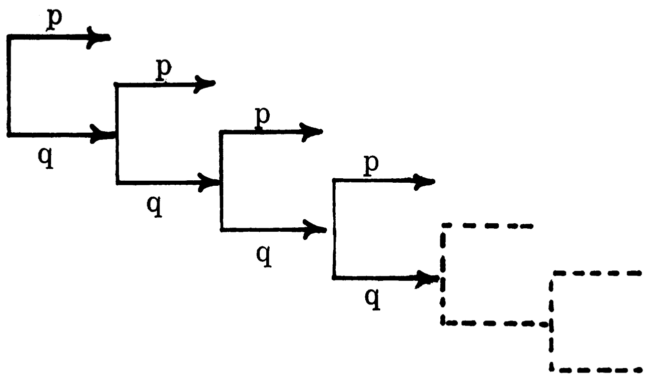

FIG. 2-1:

The entropy composition theorem now gives

$$H = H_o + qH_o + q^2 H_o + \ldots\ldots \tag{2.7}$$

where

$$H_o = -p\log p - q\log q = \frac{1}{1+\bar{m}}\log(1+\bar{m}) + \frac{\bar{m}}{1+\bar{m}}\log\left(1+\frac{1}{\bar{m}}\right) . \tag{2.8}$$

The appropriate factoring and substitution then lead to the previous expression (2. 1)

$$H = \log(1+\bar{m})+\bar{m}\log(1+\frac{1}{\bar{m}})\ \ p(0)+p(1)+p(2)+\ldots$$

$$= \log(1+\bar{m})+\bar{m}\log(1+\frac{1}{\bar{m}}) = (1+\bar{m})\log(1+\bar{m})+\bar{m}\log\frac{1}{\bar{m}} \quad . \tag{2.9}$$

The second member shows directly that if there is no noise and if the detector counts photons perfectly, a binary receiver may utilize the fraction p(0) of the wave entropy, a ternary receiver the fraction of p(0)+p(1), etc. Thus a 50 % utilization is possible with a binary receiver and an average of one photon per sample pair. A higher 'efficiency' is obtained at smaller photon counts, but at a considerably lower rate of transmission.

Figure 2-2 shows the variation of the utilization factor and rate of transmission with frequency in terms of the frequency f_o where

$$\frac{hf_o}{E_s} = \frac{hf_o}{kT_s} = 1 \quad . \tag{2.10}$$

Here E_s is the expected value of the energy per sample pair and T_s is the equivalent equilibrium temperature. This unsophisticated discussion, of course, omits the uncertainty and loss of information due to the probabilistic nature of the detection process, which was taken into account in the optimization of the binary channel in Gordon's paper[12] and in Section 2.3 of the first Interim Report[1]. This omission serves the purpose of studying as simply as possible the consequences of the structure of the 'tree' (Fig. 2-1).

In a classical description of an electromagnetic field, we may represent the time variation as :

$$e(t)=E_c(t)\cos\omega t+E_s(t)\sin\omega(t)=\sqrt{2S(t)}\cos[\omega t+\phi(t)] \tag{2.11}$$

where E_c, E_s, S and ϕ vary slowly compared to cos ωt if the bandwidth is assumed to be a small fraction of the channel frequency ω. For a maximum-entropy process, E_c and E_s are independent Gaussian random processes, S is a χ-square

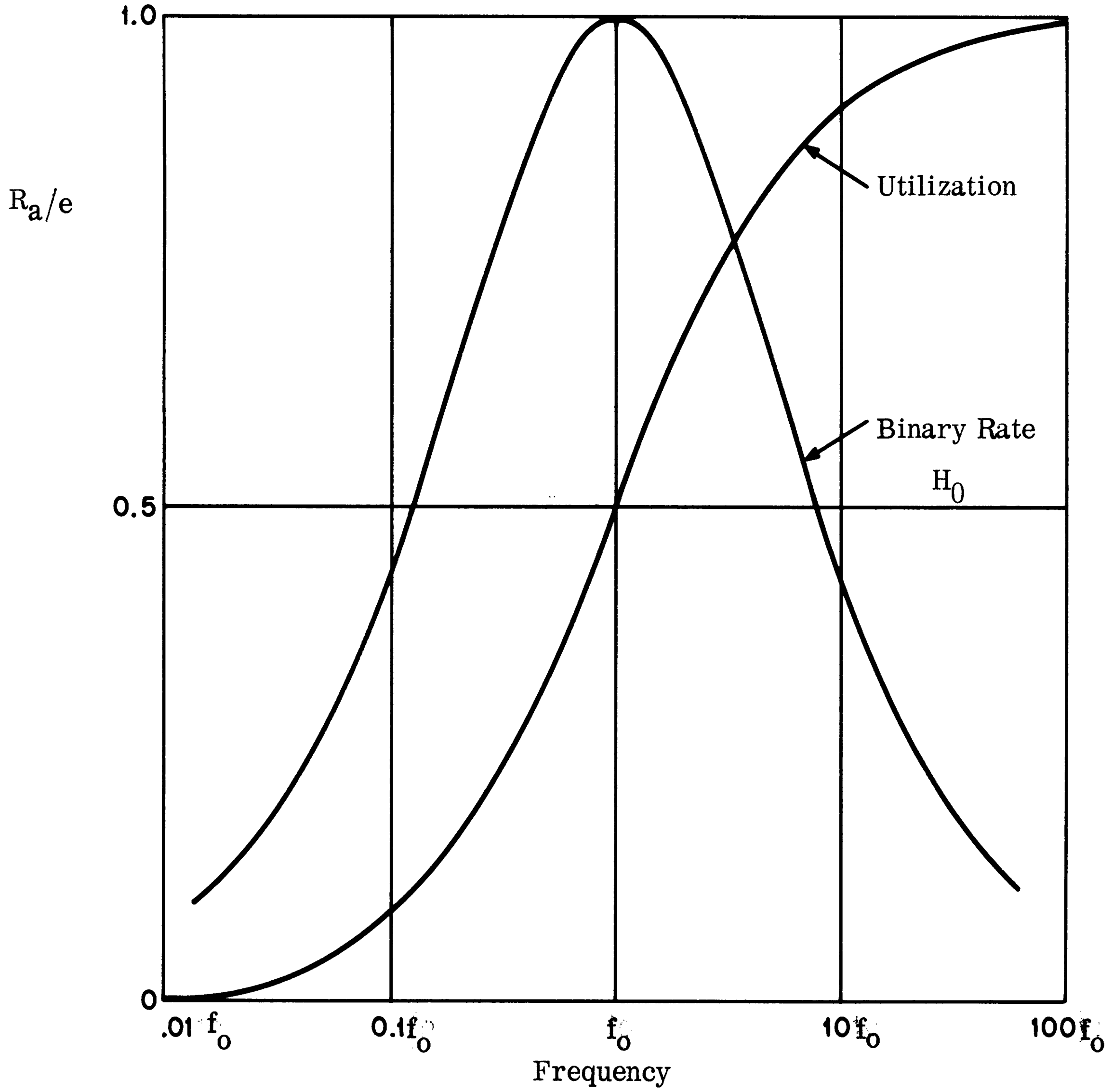

FIG. 2-2: UTILIZATION FACTOR AND RATE OF TRANSMISSION WITH FREQUENCY

process and ϕ is uniformly distributed over the 2π-interval.

Since the transformation

$$E_c = \sqrt{2S} \cos \phi \tag{2.12}$$

$$E_s = \sqrt{2S} \sin \phi \tag{2.13}$$

has a Jacobian of unity, Shannon's evaluation of the continuous distributions gives directly

$$H(E_c)+H(E_s)=H(S)+H(\phi)=\log(2\pi\psi e) \tag{2.14}$$

where ψ is the variance of e(t).

The χ-square probability density with two degrees of freedom is simply an exponential function

$$P(S)= \frac{1}{\psi} \exp\left(-\frac{S}{\psi}\right) \tag{2.15}$$

so that the entropy of S alone is very closely analogous to the entropy of the field obtained above by quantum considerations. If the S-axis is subdivided into equal infinitesimal intervals ΔS_i, the probabilities of these intervals form a geometric progression, generating a 'tree' as in Fig. 2-1. The entropy of this discrete array, except for a small readjustment of the normalizing constant, is obtained from

$$p=p(0) \cong \frac{\Delta S}{\psi} \tag{2.16}$$

$$q=1-p(0) \cong 1-\frac{\Delta S}{\psi} \tag{2.17}$$

i.e.

$$H_s=\log \frac{\psi}{\Delta S} - \left(\frac{\psi}{\Delta S}-1\right)\log\left(1-\frac{\psi}{\Delta S}\right) . \tag{2.18}$$

Here again, as ΔS approaches zero the first term grows logarithmically towards infinity, while the second term approaches the limit log e.

The result is strictly analogous to the previous quantum result; it does depend on the choice of a specific energy increment ΔS but is otherwise independent of other laws of quantum physics.

It is clear that the description of the field in terms of Gaussian components E_c and E_s does not possess such analogous properties.

2.2 Discussion of the Laser Preamplifier

The basic quantum theoretical ideas pertaining to communications channels were developed in Ref. 1. Some consideration was also given to an idealized optical communications channel. Since the case of extremely weak signals is of particular interest to us, a question naturally presents itself - - whether the use of a laser amplifier at the input end of a receiver is desirable from the information efficiency viewpoint. Some aspects of the question have been discussed by Gordon[12]. However, we shall show here that a more refined analysis is necessary before one can reach a definite conclusion.

Ideally, a laser amplifier consists of an active atomic or molecular system possessing two energy eigenstates $/2>$ and $/1>$ with energies E_2 and E_1, respectively. It is assumed that $E_2 > E_1$. If n_2 and n_1 are the populations of the respective levels, the material is said to be active when $n_2 > n_1$. The frequency of the transition $/2> \rightarrow /1>$, which is given by $(E_2 - E_1)/h$, is assumed to coincide with the midband frequency f of the channel under consideration. The bandwidth of the channel shall be denoted by Δf consistent with the notation established in Ref. 1. The amplifier is assumed to be linear.

Let S_i be the power of the input signal and N_i the noise power that may accompany it. The power output will then be

$$S_o + N_o = GS_i + GN_i + (G-1)\frac{n_2}{n_2 - n_1} hf\,\Delta f \quad , \qquad (2.19)$$

where G is the gain of the amplifier. The gain is given by

$$G = e^{a(n_2 - n_1)L} , \tag{2.20}$$

where L is the length of the active material travelled by the signal, and a is a constant characteristic of the material. Typically, it is proportional to the square of $|\langle 2/d/1\rangle|$ where d is the electric dipole moment operator of the material system. For high gain, that is for G >> 1, equation (2.19) becomes

$$S_o + N_o = GS_i + GN_i + GKhf\,\Delta f, \tag{2.21}$$

where we have introduced the quantity

$$K \equiv \frac{n_2}{n_2 - n_1} \tag{2.22}$$

which characterizes the degree of population inversion. For an active material, $n_2 - n_1 > 0$ and, therefore, $K \geq 1$. The minimum, K = 1, is attained under complete inversion; that is, when $n_1 = 0$.

The first part of the output (S_o) is to be identified with GS_i and it constitutes the amplified power of the input signal. The second part (N_o) is the sum of two terms: GN_i which results from the amplification of the noise that accompanies the signal; and GKhf Δf which represents noise generated inside the amplifier because of spontaneous emission from the upper level /2>. This second term can be thought of as arising from the amplification of an effective input noise Khf Δf. Since for an active material $K \geq 1$, the best amplifier corresponds to K=1: that is, to an active material with the lower level empty. Such an amplifier will exhibit the lowest spontaneous emission noise and the highest gain for a given number of atoms of the active material. Active materials with populations completely inverted can be created for frequencies in the microwave range. Although, to our knowledge, this has not been achieved in the infrared or optical range, we shall nevertheless consider the case K=1, since it provides an upper limit. Also it is very likely that future progress will make it feasible. Thus, for the ideal amplifier, (2.22) becomes

$$S_o+N_o=GS_i+G(N_i+hf\,\Delta f) \quad . \tag{2.23}$$

In order to investigate the information capacity of the amplified signal, recall that (equation (2.3) in Ref. 1) when the noise is much larger than hf Δf, Shannon's formula for the information capacity applies no matter how small the signal may be. From (2.23) one recognizes that N_o can be made as large as desired by making G large. Even if a single amplifier with high gain cannot be constructed (e.g. for technical reasons), one can always use several amplifiers successively so as to achieve high gain. Assuming that G is sufficiently large, the information capacity after amplification will be

$$C_{ampl}=\Delta f \log\left(1+\frac{S_o}{N_o}\right)=\Delta f \log\left(1+\frac{S_i}{N_i+hf\,\Delta f}\right) \quad . \tag{2.24}$$

The validity of this formula rests upon the assumption that the noise from spontaneous emission and the amplified input noise are additive. This has been discussed by several authors[13, 14, 15]. Under certain circumstances, it has been shown that the noise is Gaussian and additive. We feel it is worthwhile to discuss it from the point of view of the quantum formalism developed in Ref. 1 mainly in order to clarify the validity of equation (2.24).

That the noise is additive (or can be added voltage-wise as Gordon[12] remarks) implies that upon measurement of the voltage, or equivalently the field, we encounter a variance which is the sum of the variances of the various noise sources. In equation (2.29) of Ref. 1, we found that, quantum-mechanically, the variance[+] associated with a measurement of the field is

$$\sigma_q^2 = M + \frac{1}{2} - \frac{f}{h}\langle Q\rangle^2 , \qquad (2.25)$$

where M is the number of photons involved, and $\langle Q\rangle$ the expectation value of the measured field. In connection with the amplifier, M is the number of photons in its output. M can be broken up into three parts as follows:

$$M = M_1 + M_2 + M_3 , \qquad (2.26)$$

where M_1 is the number of photons in the amplified signal S_o; M_2 is the number

---

[+]Note that although σ_q is used as a measure of the uncertainty associated with a measurement of the field, it is dimensionless. In this respect, the term variance differs from the term conventionally used in probability and statistics.

of photons due to the amplified incident noise GN_i; M_3 is the number of photons due to the internally generated spontaneous emission noise. Likewise $\langle Q \rangle$ can be split into three parts $\langle Q_1 \rangle$, $\langle Q_2 \rangle$, and $\langle Q_3 \rangle$. The fields associated with the noise sources are incoherent and average to zero. Thus, $\langle Q_2 \rangle = \langle Q_3 \rangle = 0$. Equation (2.25) then becomes

$$\sigma_q^2 = \left\{ M_1 - \frac{f}{h} \langle Q_1 \rangle^2 \right\} + M_2 + M_3 + \frac{1}{2}, \tag{2.27}$$

where $\langle Q_1 \rangle$ is the field associated with the signal only. If the signal is amplified considerably so that $\langle Q_1 \rangle$ corresponds to a classical wave, then the bracketed term can be neglected as being small compared to the remaining part. Note that in writing the expectation value $\langle Q_1 \rangle$, it is assumed there is a nonvanishing field associated with the signal. The term $\frac{1}{2}$ represents the zero-point fluctuations and can be neglected as long as $M_2 + M_3$ is much larger than $\frac{1}{2}$. This is equivalent to the condition $N_o \gg hf\,\Delta f$ under which equation (2.24) is applicable. We see, therefore, that under these circumstances we encounter noise equal to $M_2 + M_3$ which is equivalent to N_o. As long as the output signal is at a classical level it is immaterial how it will be detected. One could think in terms of measuring either the field, or the energy itself. Both detection schemes will give practically the same result. Suppose now that the signal after amplification is still at a quantum level. Then, the noise is not simply N_o. In fact, if the detection scheme is based on a field measurement, a noise equivalent to $\left\{ M_1 - \frac{f}{h} \langle Q_1 \rangle^2 \right\}$ should be added. If an energy measurement is made, a term accounting for the fluctuations of the number of quanta in the signal ought to be taken into consideration. A first conclusion, therefore, is that equation (2.24) represents information capacity meaningfully only when the gain is so large that the output is a classical wave. Otherwise, the detection scheme associated with the amplifier must be specified and the problem reconsidered. The conclusion is important due to the fact that it is not a priori obvious that one will want to use a very high-gain amplifier. It might turn out that, for example, a relatively low-gain amplifier followed by a quantum counter is desirable. Moreover, the input signal may be extremely low so that even a high-gain amplifier yields an output at a quantum level.

Assuming for the moment that the conditions necessary for the validity of equation (2.24) are satisfied, we shall iterate Gordon's[12] conclusions concerning the amplifier. He defines information efficiency as the ratio of the amount of information after amplification over the information capacity of a wave with maximum entropy under the constraint of constant average power. Then, he finds that the efficiency approaches unity in the limit of large signal to noise ratio. On the other hand, for a given signal power the efficiency decreases rather rapidly after a certain frequency which depends on the power level. This is because the spontaneous emission noise becomes dominant.

Thus, as far as the spontaneous emission is concerned, one would wish to operate at as low a frequency as possible. When incident noise is also included, the results are altered quantitatively, but the general qualitative trend remains the same. Moreover, the efficiency is found to decrease when the signal power decreases.

Gordon has also compared the efficiency of the amplifier to the efficiency of a binary channel with a quantum counter as detector. From this comparison it follows that if the incident noise can be neglected, the efficiency of the amplifier becomes very small for signal levels less than approximately hf Δf. On the other hand, the efficiency of the quantum counter increases as the signal power decreases, and it approaches unity very slowly at small signal levels. However, when incident noise is included, the efficiency of the quantum counter presents a peak for a signal power of approximately one order of magnitude larger than the incident noise, and then drops off to zero. Moreover, it is found that when the number of incident noise photons is on the average greater than 0.1, the amplifier has higher efficiency. Finally, if the average number of incident signal photons is of the order of unity or larger, the efficiency of the amplifier is higher than that of the quantum counter, according to Gordon's analysis.

However, equation (2.24), upon which the foregoing analysis has been based, contains phase information as well. If the input signal is strong enough to be considered a classical wave, then it is meaningful to consider phase information at the output. But if the signal has suffered a large attenuation so that on the average only a few quanta per period arrive at the input, then, allowing for future developments, all that one can hope to know is the average number of quanta and the corresponding probability distribution. Thus, it is customary, and justified under certain conditions to assume that the probability distribution of the number of photons involved in a weak signal is a Poisson distribution. According to the formalism developed in Reference 1, this implies that we know only the diagonal matrix elements of the density operator of the field in the representation of the field. This is not a complete specification of the field since we know nothing about the off-diagonal matrix elements of the density operator, and it is those matrix elements that contain phase information. Note that this is true independently of whether we have a Poisson distribution or not, as long as all we specify is the probability distribution for the arriving photons. With such a specification for the field at the input, we have rejected phase information, and this must be taken into consideration when we examine the amount of information at the output. Thus, for a weak input signal we must invoke a more realistic description of the channel.

In principle, the phase information is contained in the density operator. If one wishes to study the effect of the amplification process on it, the off-diagonal matrix elements must be considered and their transformation due to the amplifier be found.

There is also an additional reason for which equation (2.24) is potentially unrealistic. Recall that equation (2.24) is a special case of a more general equation (see equation (2.3), Reference 1) which was derived under the assumption that the field is in a maximum entropy state. This might be true for the noise at both the input and the output, in some cases. The signal, however, is not likely to be in a maximum entropy state when it has suffered a large attenuation and subsequent amplification. For example, Stern[16] has studied the statistics of the output of a maser amplifier, assuming that the input is an exponential (maximum entropy) distribution. By using a probabilistic approach, he finds that the output is not an exponential but a much more complicated distribution which, in fact, under certain conditions reduces to a Poisson distribution. The situation will be even more involved in the case of a weak signal where one does not even have an exponential input. Of course, equation (2.24) might, presumably, still provide an upper bound but an unrealistically large one in certain cases. If, in a comparison, this upper bound is smaller than what it is compared to, the amplifier is excluded. Otherwise, a different approach is necessary.

The foregoing considerations point to the need for a more realistic analysis of the amplification process and the information efficiency of a laser amplifier used in a communication channel. Again, the whole difficulty stems basically from the fact that, in dealing with quantum phenomena, one must know what is to be measured. This in turn implies that one must specify how the amplifier is going to be used in the channel. Subsequently, we develop the formalism for the study of a specific communication channel which utilizes a laser amplifier. Let it be noted in advance that if the incident noise were zero, the amplifier could not improve the situation. It is because of the existence of incident noise, that the amplifier might be expected to be useful. In addition, the laser amplifier may serve simultaneously as a filter and reduce the total amount of noise reaching the detector.

2.3. Binary Channel with Preamplifier

For a communication channel involving a weak signal in which the average number of photons per sample is small, a binary channel appears to be a rather natural choice. Such a channel with no background noise and with a quantum counter as a detector was analyzed in Ref. 1. Here, we consider a binary channel with a weak signal accompanied by noise. This signal constitutes the input of a laser amplifier whose output is detected by a threshold detector.

Let R be the threshold of the detector. If R or more photons are received, a [1] is recorded. . Otherwise, a [0] is recorded.

Let $W^{SN}(n)$ be the probability that n photons arrive at the input of the amplifier when [1] is transmitted, and $W^{N}(n)$ the probability that n photons arrive when [0] is transmitted. In the first case the photons are due to the signal and the incident noise, while in the second case they are solely due to the incident noise. If $W^{S}(n)$ is the probability that n <u>signal</u> photons arrive, we shall have

$$W^{SN}(n) = \sum_{m=0}^{n} W^{S}(m)\, W^{N}(n-m) \tag{2.28}$$

Let $W^{A}(n;m)$ be the probability that m photons will appear in the output of the amplifier, when it is known that exactly n photons entered the input. Then, the probability $W^{SNA}(m)$ that m photons will arrive at the detector when [1] is transmitted is

$$W^{SNA}(m) = \sum_{n=0}^{\infty} W^{SN}(n)\, W^{A}(n;m). \tag{2.29}$$

Similarly, the probability $W^{NA}(m)$ that m photons will arrive at the detector when [0] is transmitted is[+]

$$W^{NA}(m) = \sum_{n=0}^{\infty} W^{N}(n)\, W^{A}(n;m). \tag{2.30}$$

[+] The superscripts S, N, and A correspond to signal, incident noise and amplifier respectively.

Extending the summation in equations (2.29) and (2.30) up to ∞ implies that we assume that there is a finite probability for less photons to appear in the output than entered the input of the amplifier. In principle, this is possible. However, on physical grounds and according to the results of Shimoda, et al[17], at least for the case of an amplifier with high gain, we may assume that

$$W^A(n; m) = 0 \quad \text{for } m<n. \tag{2.31}$$

Then, equations (2.29) and (2.30) become

$$W^{SNA}(m) = \sum_{n=0}^{m} W^{SN}(n)\, W^A(n; m), \tag{2.32}$$

and

$$W^{NA}(m) = \sum_{n=0}^{m} W^N(n)\, W^A(n; m). \tag{2.33}$$

Let now $V^{SNA}(R)$ be the probability that less than R photons will arrive at the detector when [1] is transmitted. Then we shall have

$$V^{SNA}(R) = \sum_{m=0}^{R-1} W^{SNA}(m) =$$

$$= \sum_{m=0}^{R-1} \sum_{n=0}^{m} W^{SN}(n)\, W^A(n; m), \tag{2.34}$$

which by virtue of equation (2.28) also reads

$$V^{SNA}(R) = \sum_{m=0}^{R-1} \sum_{n=0}^{m} \sum_{r=0}^{n} W^S(r) W^N(n-r)\, W^A(n; m). \tag{2.35}$$

The probability for R or more photons to arrive at the detector when [1] is transmitted is $1 - V^{SNA}(R)$.

Similarly, the probability that less than R photons will arrive at the detector when [0] is transmitted is

$$V_0^{NA}(R) = \sum_{m=0}^{R-1} W^{NA}(m) = \sum_{m=0}^{R-1} \sum_{n=0}^{m} W^{N}(n) W^{A}(n;m) \tag{2.36}$$

and the probability that R or more photons will arrive at the detector when [0] is transmitted is

$$1 - V_0^{NA}(R) .$$

Following Ref. 1, let Q be the probability of a transmitted pulse. Moreover, we introduce the symbols

$$p \equiv 1 - V^{SNA}(R) \quad , \tag{2.37}$$

$$q \equiv 1 - V_0^{NA}(R) \quad . \tag{2.38}$$

We also introduce the function $F[X]$ defined by

$$F[X] = X \log X^{-1} \quad . \tag{2.39}$$

Then the probability matrix, (equation (2.36), Ref. 1) is

$$\begin{vmatrix} P(1,1) & P(0,1) \\ P(1,0) & P(0,0) \end{vmatrix} = \begin{vmatrix} Qp & (1-Q)q \\ Q(1-p) & (1-Q)(1-q) \end{vmatrix} \quad . \tag{2.40}$$

Furthermore, applying equation (2.35) of Ref. 1, we find that the rate of transmission of information per sample is

$$C = F\left[Q(1-p)+(1-Q)(1-q)\right] + F\left[Qp+(1-Q)q\right] - Q\left\{F[1-p] + F[p]\right\} - (1-Q)\left\{F[1-q] + F[q]\right\} \quad . \tag{2.41}$$

Note that equation (2.35) of Reference 1 is recaptured as a special case of equation (2.41) by setting $q = 0$ and $R = 1$. Here, q is not zero because of the presence of incident noise and spontaneous emission from the amplifier. To calculate C, one needs to know the probability distributions W^N, W^S and W^A which we discuss subsequently.

We are interested in signals which originate from some distant source and have suffered a large attenuation. If the attenuation is a random process, we may assume that the identity of the source has been washed out and take the distribution $W^S(n)$ to be a Poisson distribution, as long as the signal is weak. Let S be the expected number of arriving photons per sample. Then

$$W^S(n) = \frac{S^n e^{-S}}{n!} . \tag{2.42}$$

Also, as long as the incident noise is not going to be very strong, we may assume that the probability distribution $W^N(n)$ is a Poisson distribution. Let its average be N. Then

$$W^N(n) = \frac{N^n e^{-N}}{n!} . \tag{2.43}$$

Since the Poisson distribution is additive, we shall have

$$W^{SN}(n) = \frac{M^n e^{-M}}{n!} , \tag{2.44}$$

where

$$M \equiv S + N, \tag{2.45}$$

and it represents the average number of signal-plus-noise photons per sample.

Shimoda et al.[17] have shown that for an ideal amplifier (i.e. $K = 1$) with high gain (i.e. $G \gg 1$) the probability distribution $W^A(n; m)$ is

$$W^A(n; m) = \frac{1}{G}\left(\frac{m}{G}\right)^n \frac{e^{-m/G}}{n!}, \quad \text{for } m \geq n \tag{2.46}$$

$$= 0 \quad \text{for } m < n$$

The above equation is valid under the assumption that G does not depend on frequency, and that it does not fluctuate due, for example, to variations in pumping.

Introducing, for the sake of notational simplicity, the quantity

$$g \equiv \frac{1}{G}, \tag{2.47}$$

we have:

$$V^{SNA}(R) = ge^{-M} \sum_{m=0}^{R-1} \sum_{n=0}^{m} \frac{M^n}{(n!)^2} (gm)^n e^{-gm}, \tag{2.48}$$

$$V_o^{NA}(R) = ge^{-N} \sum_{m=0}^{R-1} \sum_{n=0}^{m} \frac{N^n}{(n!)^2} (gm)^n e^{-gm} \tag{2.49}$$

As already mentioned, $V_o^{NA}(R)$ accounts for the incident noise and the spontaneous emission noise. The case of zero incident noise is obtained for $N = 0$. The case of nonvanishing incident noise without amplifier has been examined by Gordon[12]. The next step, therefore, will be to compare the rate of transmission of information without amplifier, to the rate of transmission of information with amplifier, on the basis of equation (2.41). Clearly, for the cases in which Gordon's results predict that the amplifier's efficiency is lower than that of the noisy binary channel with a quantum counter, no further consideration is necessary since the amplifier's efficiency is overestimated. Thus, the amplifier is ruled out in those cases. Otherwise, a comparison based on equation (2.41) and the probability distributions exhibited above is necessary, before one can reach a final conclusion about the usefulness of the amplifier. Such a comparison will be our objective in the next period.

III. Third Problem Area: Optical Bandpass Filters

3.1. The Wernicke Prismatic Filter

A prism-type filter was discussed in the first Interim Report[1]. It was suggested that this filter, which has the geometrical configuration of the Wernicke prism, has some possible potential for tuning. This section of the report discusses the transmission characteristics of this filter and the practicality of tuning it.

3.2. Development of Filter Transmissivity and Calculations.

The filter configuration is shown in Fig. 3-1 with the dimensions and other parameters indicated. The refractive indices of the two materials of which the prism is made are n_1 and n_2. In this development, we will assume there is an entrance slit of height 2H through which passes a parallel beam of light. Light which is reflected out of the primary beam within the prism will be assumed to be absorbed at the walls so that no secondary beams are considered. Absorption within the prism is neglected for simplicity; it will be discussed later.

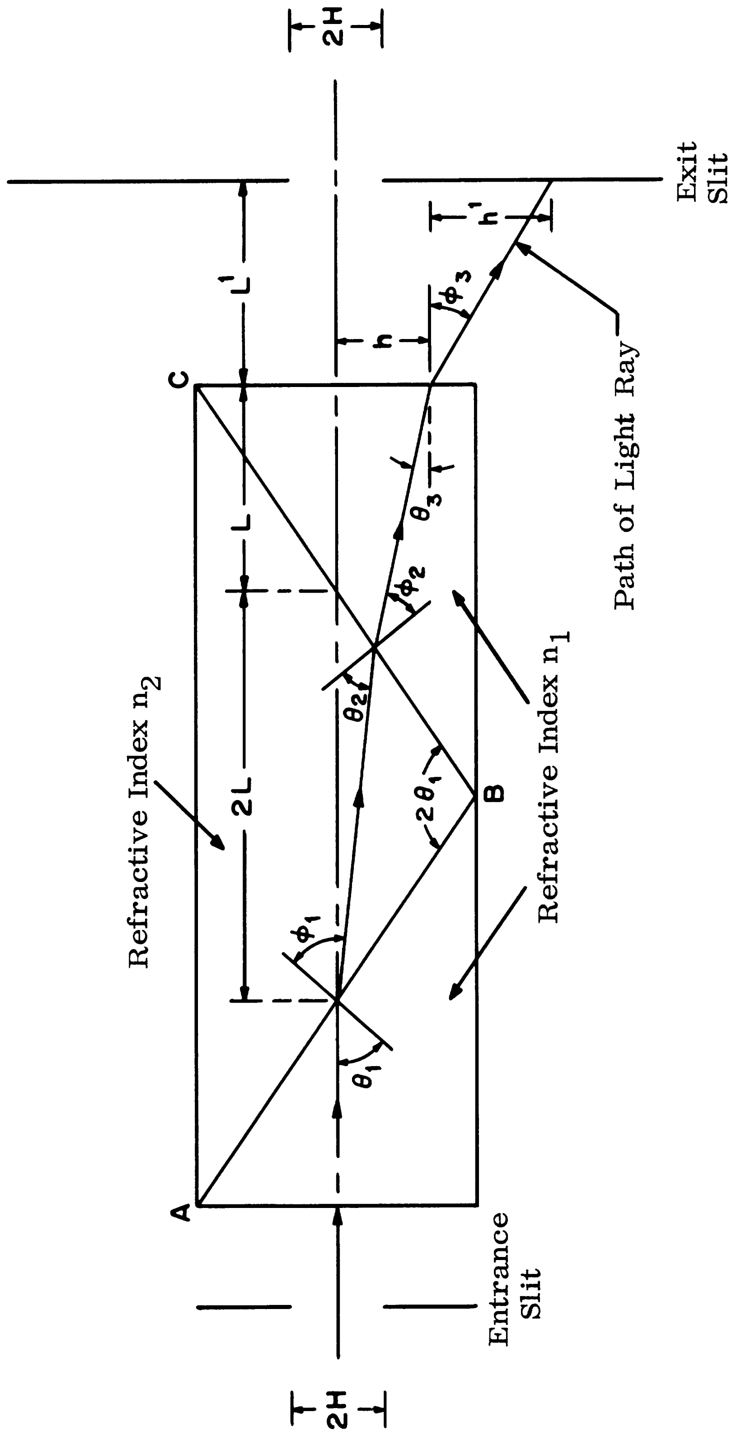

FIG. 3-1: DIAGRAM OF THE WERNICKE FILTER

Diffraction effects at the entrance and exit slits are also neglected. The light will be assumed to be polarized with the electric vector parallel to the entrance slit. The Gaussian system of units is used.

Light which is normally incident on the first air-glass interface will be partially reflected, and the amplitude E_{t1} of the transmitted electric vector will be, for unit incident amplitude,

$$E_{t1} = \frac{2n_o}{n_1 + n_o}. \tag{3.1}$$

At AB where the light falls obliquely on the interface, the transmitted amplitude is given by

$$E_{t2} = \frac{E_{t1}\, 2n_1 \cos\theta_1}{n_1 \cos\theta_1 + n_2 \cos\phi_1} \tag{3.2}$$

and from Snell's law we have

$$n_1 \sin\theta_1 = n_2 \sin\theta_2 \tag{3.3}$$

The amplitude of the transmitted electric vector at the remaining interfaces is found in a similar manner, so that the electric vector of the emerging wave is given by

$$E_{to} = \frac{2^4\, n_o\, n_1^2\, n_2 \cos\theta_1 \cos\theta_2 \cos\theta_3}{\left[(n_1+n_o)(n_1\cos\theta_1 + n_2\cos\phi_1)(n_2\cos\theta_2 + n_1\cos\phi_2)(n_1\cos\theta_3 + n_o\cos\phi_3)\right]} \tag{3.4}$$

where

$$\phi_1 = \sin^{-1}\left[\frac{n_1}{n_2}\sin\theta_1\right] \tag{3.5}$$

$$\theta_2 = 2\theta_1 - \phi_1 \tag{3.6}$$

$$\phi_2 = \sin^{-1}\left[\frac{n_2}{n_1} \sin\theta_2\right] \tag{3.7}$$

$$\theta_3 = \theta_1 - \phi_2 \tag{3.8}$$

$$\phi_3 = \sin^{-1}\left[\frac{n_1}{n_o} \sin\theta_3\right] \tag{3.9}$$

In order to obtain the intensity of the output light, we square the amplitude of the electric vector as given by (3.4) and multiply by the ratio of the cosine of the angle of incidence to the cosine of the angle of transmission and the ratio of the refractive indices at each interface to find the power flow through the interfaces, and obtain

$$I_o = \frac{E_{to}^2 \cos\phi_1 \cos\phi_2 \cos\phi_3}{\cos\theta_1 \cos\theta_2 \cos\theta_3} \tag{3.10}$$

The refractive index terms which appear in the power flow expression have cancelled out.

The light power passed by the exit slit will be further decreased due to the dispersive effect of the prism. If h is the total displacement of the beam, then the total light power passed by the exit slit will be

$$P_o = I_o\left(1 - \frac{h}{2H}\right) A \tag{3.11}$$

where we have assumed an exit slit of the same height as the entrance slit and A is the area of both slits. The displacement of the output light beam is found to be

$$h = \frac{L}{\sin\theta_1}\left\{\left[3\sin\theta_1 - \frac{\cos(\theta_1-\theta_2)\sin 2\theta_1}{\cos\theta_2}\right]\tan\theta_3 + \frac{\sin 2\theta_1}{\cos\theta_2}\sin\left|\theta_1-\theta_2\right|\right\} \qquad (3.12)$$

This displacement is measured with respect to the point at which an undeflected ray would emerge from the filter, and is taken to be positive in either direction from the undeflected position. If the exit slit is located a distance L^1 from the last glass-air interface, then an additional displacement h^1 results,

$$h^1 = L^1 \tan\phi_3 \qquad (3.13)$$

Finally then if the ratio of the output to input power is formed, the power transmission coefficient τ is obtained, as

$$\tau = I_o\left[1 - \frac{h+h^1}{2H}\right] \qquad (3.14)$$

where now I_0 is dimensionless, since we have divided by the power in the incident field. When this expression becomes negative, the output is then, of course, zero.

Some calculations have been carried out for the Wernicke filter as a function of the ratio $\frac{n_1}{n_2}$, for an angle θ_1 of 60^o and a ratio $\frac{n_1}{n_o}$ of 1.5. Figure 3-2 shows the quantity I_o as $\frac{n_1}{n_2}$ is varied. The transmission abruptly goes to zero when $\frac{n_1}{n_2} = 1.152$ since then the light no longer is incident

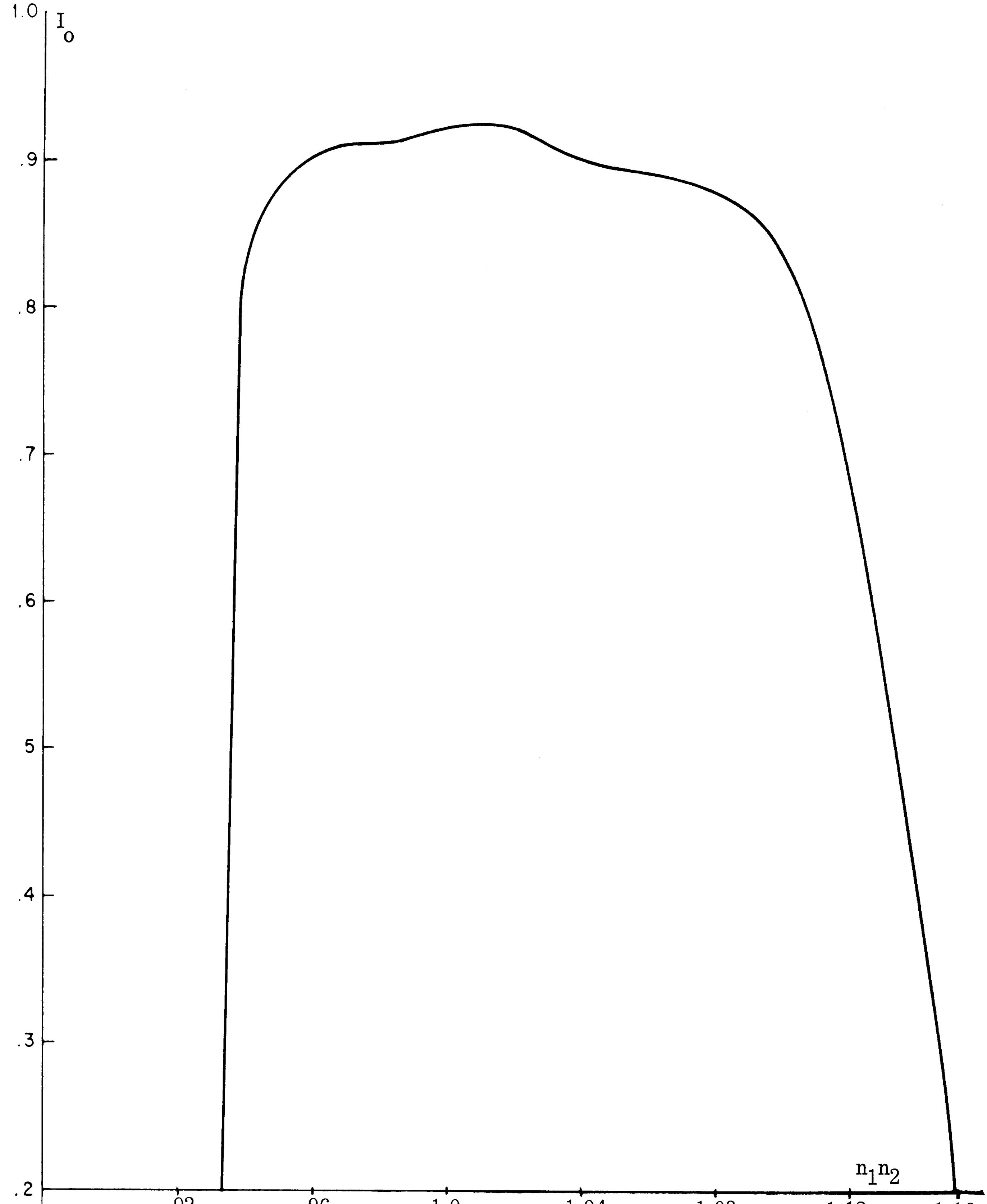

FIG. 3-2: TRANSMITTED LIGHT INTENSITY, I_o, AS FUNCTION OF n_1/n_2=1.5

on the exit face of the prism, but strikes the bottom surface. Figs. 3-3 and 3-4 show the displacement ratios $\frac{h_o}{L}$ and $\frac{h_o^1}{L^1}$ as $\frac{n_1}{n_2}$ varies. By utilizing

the results of these graphs we can find the power transmission coefficient of the filter as a function of $\frac{n_1}{n_2}$. We are primarily interested in however, the filter transmission as the frequency is varied, so that we must assume some model for the frequency dependence of n_1 and n_2 on f. For simplicity it has been assumed that

$$n_{1,2}(f) = n_c \left[1 + \Delta \tan \alpha_{1,2}\right] \tag{3.15}$$

where n_c is the common refractive index of both parts of the filter at the center frequency of the passband, and Δ is the fractional change in the frequency about the center frequency; i.e.,

$$\frac{f - f_c}{f_c} = \Delta \tag{3.16}$$

Since

$$\frac{f_c}{n_c} \frac{dn}{df} = \tan \alpha$$

it is apparent that $\tan \alpha$ is a measure of the sensitivity of n to changes in f.

The bandwidth of the filter is now defined to be the frequency separation of the half-power points with respect to the maximum transmission

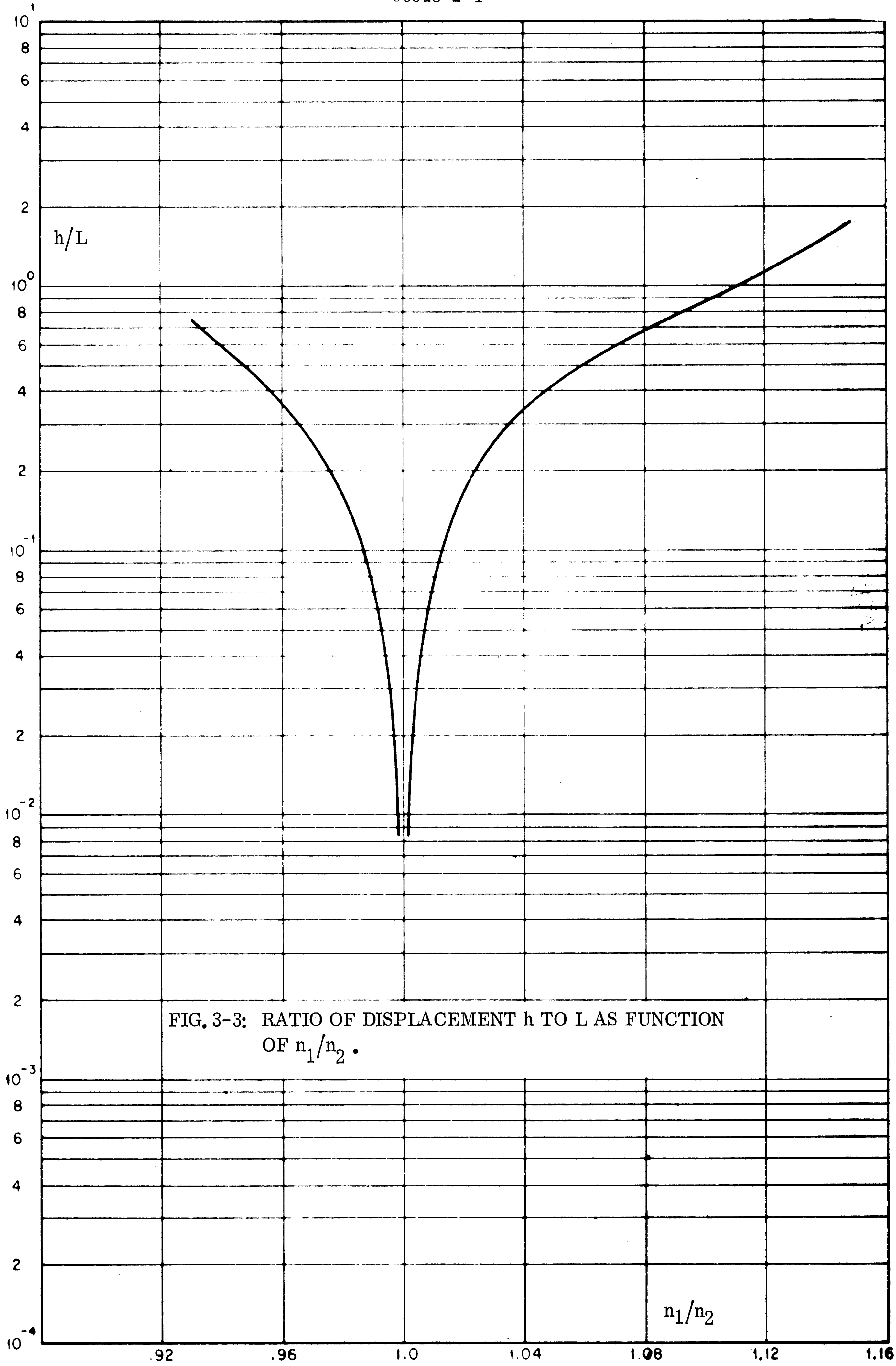

FIG. 3-3: RATIO OF DISPLACEMENT h TO L AS FUNCTION OF n_1/n_2.

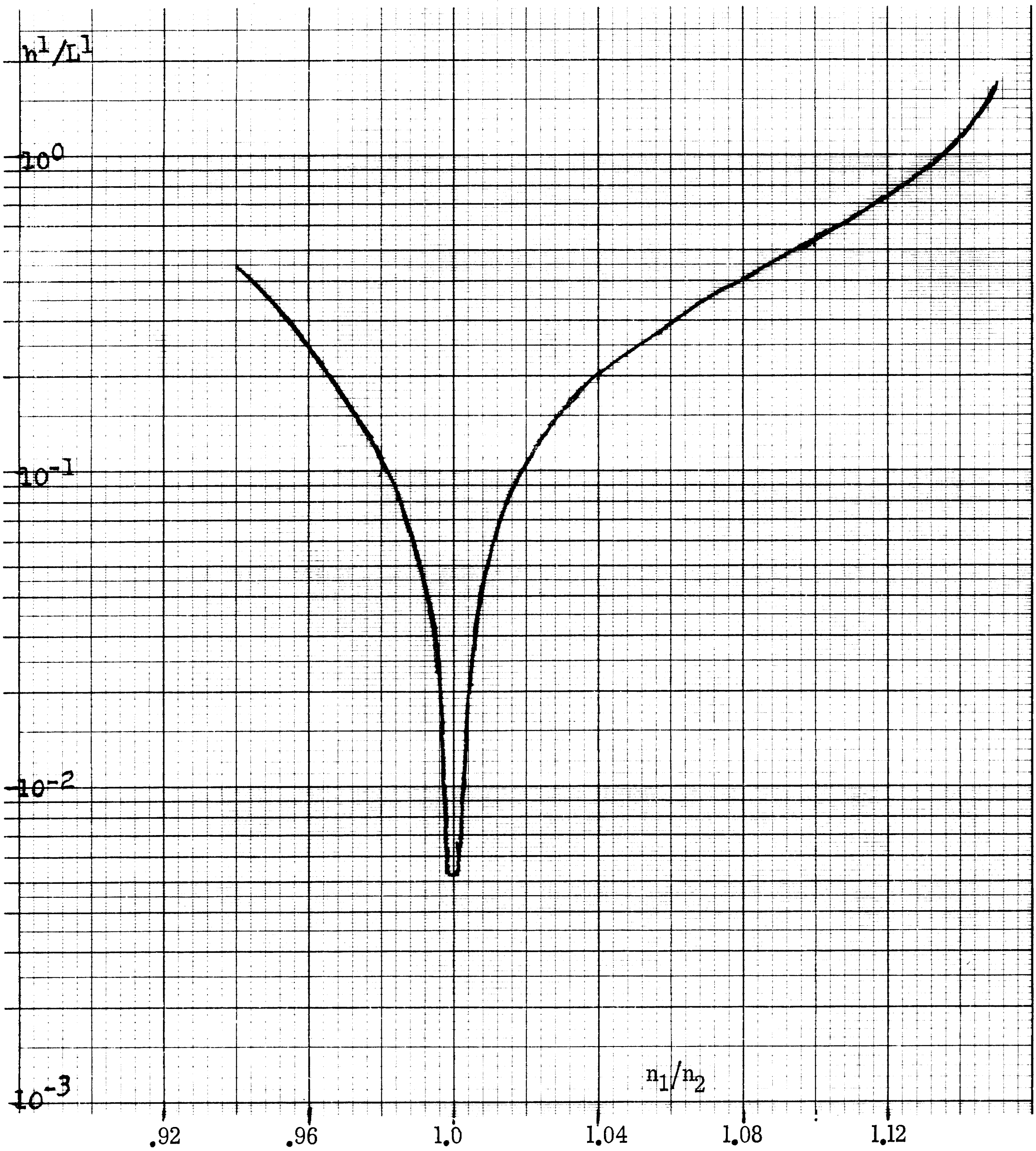

FIG. 3-4: RATIO OF DISPLACEMENT h^1 TO L^1 AS FUNCTION OF n_1/n_2

and the normalized bandwidth N_B is taken to be the bandwidth divided by the center frequency. We can write the normalized bandwidth N_B, as

$$N_B = \frac{f_U - f_L}{f_c} = \Delta_U - \Delta_L = \frac{(n_1/n_2)_U - 1}{\tan\alpha_1 - \left(\frac{n_1}{n_2}\right)_U \tan\alpha_2} - \frac{(n_1/n_2)_L - 1}{\tan\alpha_1 - \left(\frac{n_1}{n_2}\right)_L \tan\alpha_2} \tag{3.17}$$

where f_U and f_L are the upper and lower frequencies of the pass bands, and $(n_1/n_2)_U$ and $(n_1/n_2)_L$ are the ratios of (n_1/n_2) when the transmitted power has fallen to one-half at the frequencies f_U and f_L. It should be noted that $-1 < \Delta_L < 0$ and $0 < \Delta_U < \infty$ so that $0 < N_B < \infty$. This presents an unrealistic picture when $N_B > 1$ since the concept of a normalized bandwidth then becomes somewhat meaningless. Actually, a normalized bandwidth greater than 1 is of no interest here and we will devote our attention primarily to values of $N_B < 1$.

Since n_1/n_2 is symmetric about 1.0 over the range of values used in the calculations below, then (3.17) can be simplified to

$$N_B = \frac{2\,\delta}{\tan\alpha_1} = \frac{2}{\tan\alpha_1}\left[(n_1/n_2)_U - 1\right] \tag{3.18}$$

where $\tan\alpha_2$ has been set zero for simplicity, and

$$(n_1/n_2)_U = 1.0 + \delta; \quad (n_1/n_2)_L = 1.0 - \delta \quad . \tag{3.19}$$

The quantity $(n_1/n_2)_U$ can now be obtained from (3.14), noting that τ is reduced to one-half its maximum value when

$$\frac{h+h^1}{2H} = \frac{1}{2} \quad . \tag{3.20}$$

An approximate value for $(n_1/n_2)_U$ can then be calculated for the range $.995 \leq n_1/n_2 \leq 1.005$ by noting that the expressions,

$$\frac{h^1}{L^1} = \pm b^1 \left(\frac{n_1}{n_2} - 1\right) ; \quad \frac{h}{L} = \pm b \left(\frac{n_1}{n_2} - 1\right) , \tag{3.21}$$

are approximately true, where b and b^1 are the slopes of the h/L and h^1/L^1 curves, the + sign applying for $n_1/n_2 > 1.0$, and the - sign for $n_1/n_2 < 1.0$. As a result of (3.18) and (3.21) we obtain then

$$Lb \left[(n_1/n_2)_U - 1\right] + L^1 b^1 \left[(n_1/n_2)_U - 1\right] = H \quad . \tag{3.22}$$

Thus,

$$(n_1/n_2)_U - 1 = \frac{H}{Lb + L^1 b^1} \tag{3.23}$$

and

$$N_B = \frac{2}{\tan \alpha_1 \left[\frac{Lb}{H} + \frac{L^1 b^1}{H}\right]} \quad . \tag{3.24}$$

This expression is valid when (3.21) holds, or when $N_B \tan \alpha < .01$. In that case, since $b \approx 8$ and $b^1 \approx 5$, $8 \frac{L}{H} + 5 \frac{L^1}{H} \geq 200$ is required. It may be seen from (3.24) that N_B decreases inversely proportional to L/H and L^1/H so that the ability to achieve sharper filter characteristics by increasing these parameters is limited by the largest practical L and L^1 and smallest practical H which could be used.

The normalized bandwidth for this filter is shown in Figs. 3-5 to 3-7 as a function of L/H, L^1/H and $\tan \alpha_1$, obtained without approximation from Figs. 3-3 and 3-4 and expression (3.18). It should be noted that values of L/H

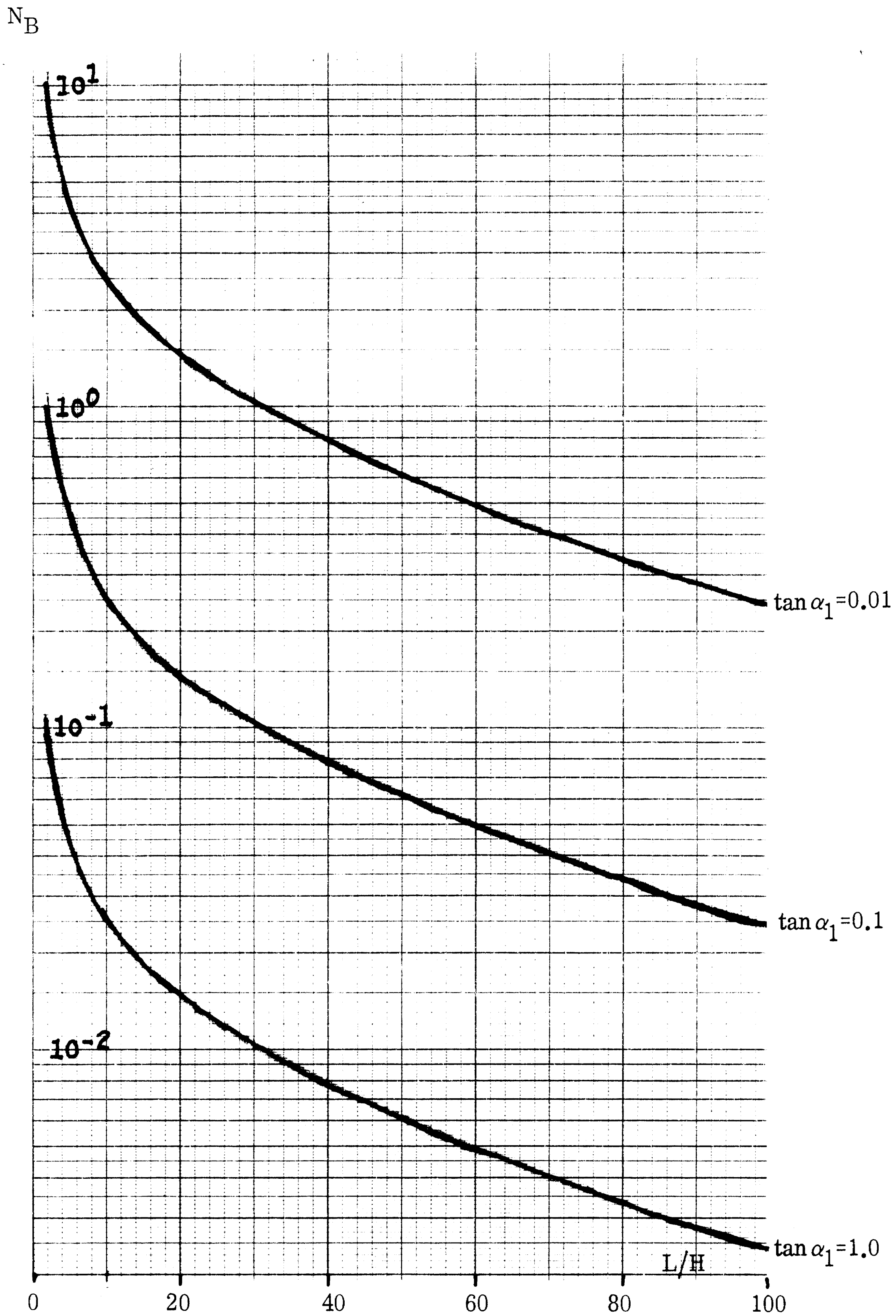

FIG. 3-5: NORMALIZED BANDWIDTH N_B FOR L^1 AND $\tan\alpha_2 = 0$ AS A FUNCTION OF L/H AND $\tan\alpha_1$

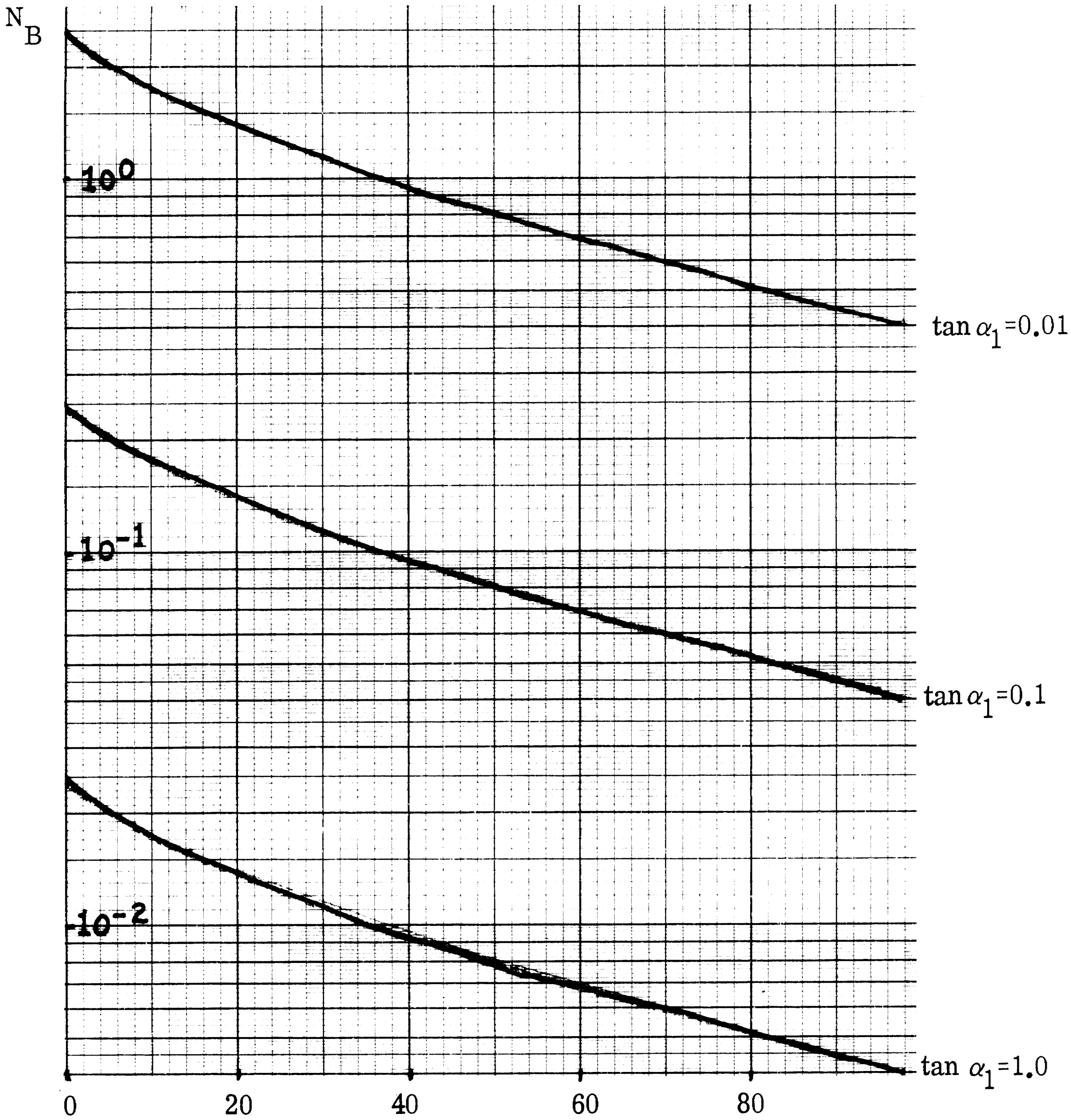

FIG. 3-6: NORMALIZED BANDWIDTH N_B FOR $\tan\alpha_2=0$ AND L/H=10 AS A FUNCTION OF L^1/H AND $\tan\alpha_1$.

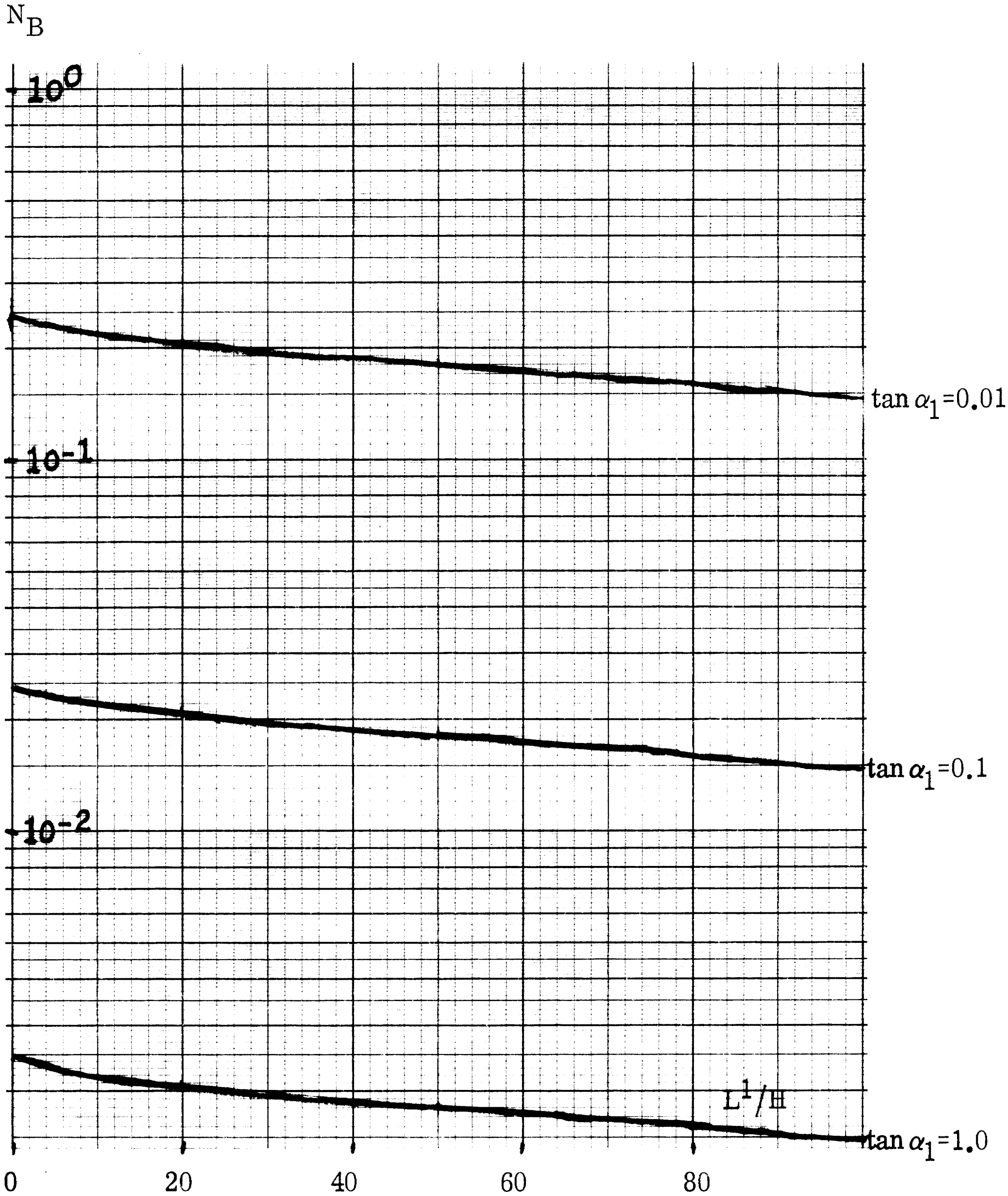

FIG. 3-7: NORMALIZED BANDWIDTH N_B FOR $\tan\alpha_2$=0 and L/H=100 AS A FUNCTION OF L^1/H AND $\tan\alpha_1$

less than tan θ_1 are not meaningful since then, as can be determined by Fig. 3-1, the entrance and exit slits would extend below the apex of the center prism and light could pass through the two slits without having encountered it. Since θ_1 is 60^o for these curves, then $L/H > 1.73$

Recalling that the intended application for this filter would be in a laser communication system with a frequency range from $1.5x10^{13}$ to $7.5x10^{14}$ cps and a bandwidth of 10^9 cps, it is apparent that the Wernicke filter is unsuited for this application, since the required value of N_B is $6.6x10^{-5}$ to $1.33x10^{-6}$. This is 3 to 4 orders of magnitude less than what can be achieved with a reasonable value for tan α and L/H. Actually, almost any value of N_B that was desired could be obtained by choosing tan α large enough, but some data on materials used in this frequency range given by Kruse[2] indicates that the maximum value for tan α may be on the order of 0.1. This value leads to normalized bandwidths on the order of 10^{-2}. Usually, materials that are more dispersive are also more lossy so that the insertion loss of the filter could be intolerably large. It should be recalled that Fig. 3-2 shows the maximum transmissivity of the filter considered in these calculations is about 90 $^o/_o$, but absorption has been neglected.

The normalized bandwidth could be decreased by increasing the angle θ_1. In the idealized treatment made here, this would indicate an improved filter performance. However, because the normalized bandwidth when θ_1 is 60^o has been found to be 3 to 4 orders of magnitude larger than what is required, and losses in a real filter would further decrease its effectivness, there seems to be no advantage to calculating the filter performance for other values of θ_1.

Tuning of this filter could be achieved in principle if one of the materials of which the filter is constructed were electro-optic in nature. However, the electro-optic coefficient for potassium dihydrogen phosphate (KDP), a material with a relatively large electro-optic coefficient of 8.47×10^{-12} meter/volt (Peters[19]), leads to a change in the refractive index of only $25 \times 10^{-12} E$, where E is the electric field in volts/meter. Thus, even for very large field strengths, only a very small refractive index change takes place, with negligible change in the center frequency of the filter.

Actually, the requirement for tunability of the filter would then be that the refractive indices of the two materials comprising the filter have very nearly the same frequency dependence, so that the crossover point could be changed greatly by a small change in either refractive index. On the other hand, in order to achieve a narrow band pass the frequency characteristics of the refractive indices of the two materials should be very different. These two requirements are thus not compatible.

3.3 The Polarization Interference Filter

The polarization interference filter, or as it is also known, the Lyot-Öhman filter and birefringent filter is a particularly attractive one from the standpoint of the narrowness of the obtainable bandwidth and the possibility of tuning it. This filter was designed by Lyot[20] and first built by Öhman[21]. In this report, the various features of this filter are discussed and its applicability in a laser communication channel is considered.

3.4. Bandwidth and Transmission Characteristics of the Polarization Interference Filter

The polarization interference filter may take different forms. Evans[22] considers several possibilities. The discussion here is limited to the most basic of these forms which consists of sections of birefringent plates cut with their optic axes parallel to the large faces of the plates and placed between polarizers oriented at 45° to the optic axes. A diagram of the filter is shown in Fig. 3-8.

The mechanism on which the filter operation depends is the difference in propagation velocity for ordinary and extraordinary waves in the birefringent material. When a linearly polarized wave is incident at 45° to the optic axis of the birefringent material, the beam is split into two waves, the ordinary and the extraordinary wave. The beams

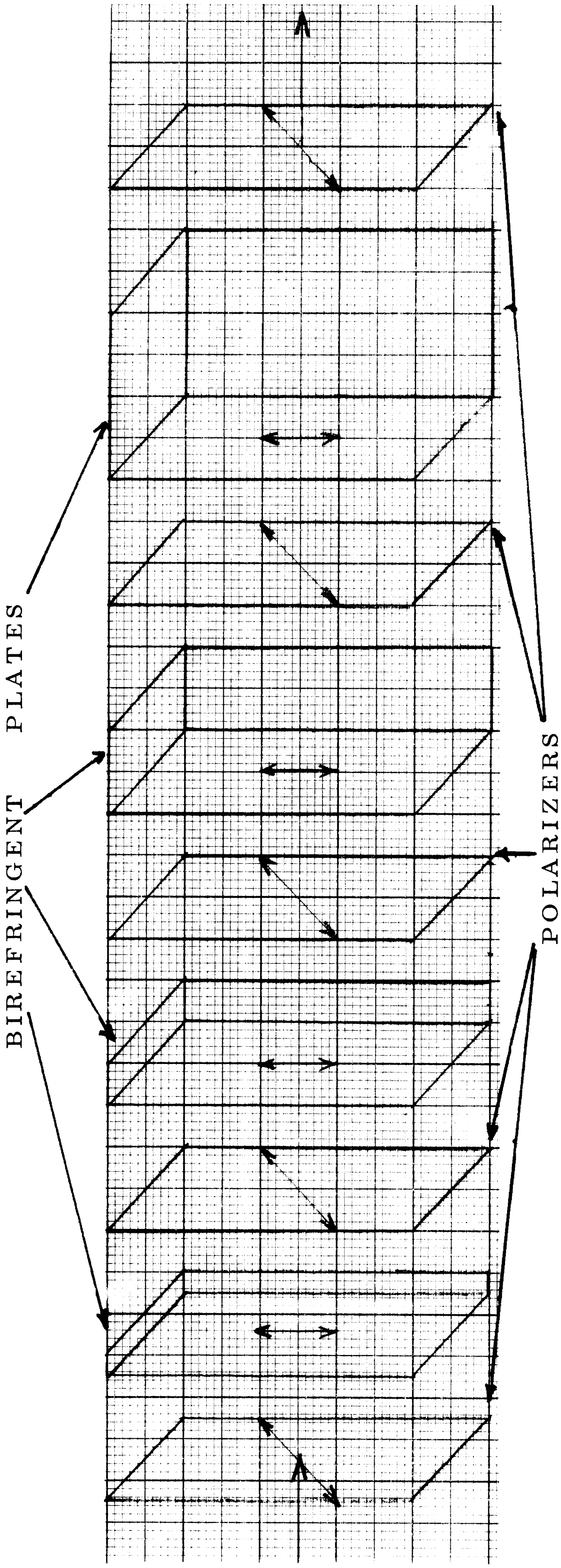

FIG. 3-8: POLARIZATION INTERFERENCE FILTER.
Arrows show orientation of optic axes of birefringent plates and polarizers.

emerge from the birefringent material polarized at right angles and with a phase difference depending on the difference in velocity of propagation. The amplitude of the wave transmitted by a second polarizer depends on the relative retardation of the two beams. If the difference in retardation is an integral number of half waves, the interference between the waves is destructive, and no transmission occurs. For the single birefringent plate of thickness d placed between parallel polarizers, where absorption within the plate and reflection losses are neglected, the transmission is given by Billings, et al[23] as

$$T_1 = \cos^2 \left[\frac{\pi d \mu}{\lambda} \right] \tag{3.25}$$

where $\mu = n_e - n_o$

and n_e and n_o are the extraordinary and ordinary indices of refraction at wavelength λ. When white light is incident on such a plate and polarizer arrangement and the output is observed by a spectrograph, a series of bright and dark bands, which is called a channel spectrum, is obtained. This results from the argument of the cosine above taking on integral values representing the higher order interference fringes.

If several sections of these plates are put together as shown in Fig. 3-8, and the thicknesses of birefringent plates are adjusted in the ratios 1, 2, 4, etc., the overall transmission characteristic of such an arrangement exhibits pass bands whose widths are equal to the fringe widths of the thickest plate separated in wave length by the distance between fringes of the thinnest plate. If the sections are numbered $i = 1, \ldots, N,$ the ith section will have a thickness

$$d_i = 2^{i-1} d_1$$

$$d_N = 2^{N-1} d_1$$

where d_1 is the thickness of section 1. The transmission of the whole system can then be given, when the absorption is ignored, by

$$T = \left[\cos\theta \cos 2\theta \cos 4\theta \ldots \cos 2^{N-1}\theta\right]^2 \tag{3.26}$$

where $\theta = \frac{\pi d\mu}{\lambda}$

is 1/2 the angular retardation of section 1. The retardation is also spoken of in waves, and is given by

$$\Gamma_\lambda = \frac{d}{\lambda}\mu \quad .$$

Thus, in order for the whole array to have a common transmission peak, the retardation of each section in waves must be an integer such that with

$$\Gamma_i = n_i ; \; \Gamma_1 = n_1 \quad ,$$

$$n_i = 2^{i-1} n_1 \quad .$$

There are also side band peaks centered about the main peak and separated from it by the fringe width of the thickest section.

Billings[24] showed that (3.26) can be written as

$$T = \left[\frac{\sin 2^N\theta}{2^N \sin\theta}\right]^2 \tag{3.27}$$

Figure 3-9 shows a plot of this function. It may be observed that this curve resembles that of the familiar $(\frac{\sin x}{x})^2$ function encountered in diffraction theory. When the amount of light energy transmitted by the filter between the pass bands is calculated, it is found to be 0.11 of that contained in the pass band Evans[22]. Thus if an auxillary wide-band filter were to be used to remove the unwanted transmission bands on either side of the desired one, the background light transmitted by the polarization filter would be essentially confined to the main pass band.

The band width B of the filter is, as mentioned above, determined by thickest plate in the filter, and is(Billings)[23], at the half power points given by

$$B_\lambda = \frac{0.5\,\lambda_o^2}{2^{N-1}\,d_1\mu} = \frac{0.5\,\lambda_o^2}{d_N\mu} \tag{3.28}$$

in terms of the wave length. λ_o is the position of the pass band. The normalized band width N_B is defined to be the band width to center wave length ratio, or

$$N_B = \frac{0.5\,\lambda_o}{2^{N-1}\,d_1\mu} = \frac{0.5\,\lambda_o}{d_N\mu} \tag{3.29}$$

Thus for a given normalized band width, the filter dimension will be proportional to the wave length. If,instead, it is desired that the band width be given in terms of the frequency, then with c the velocity of light

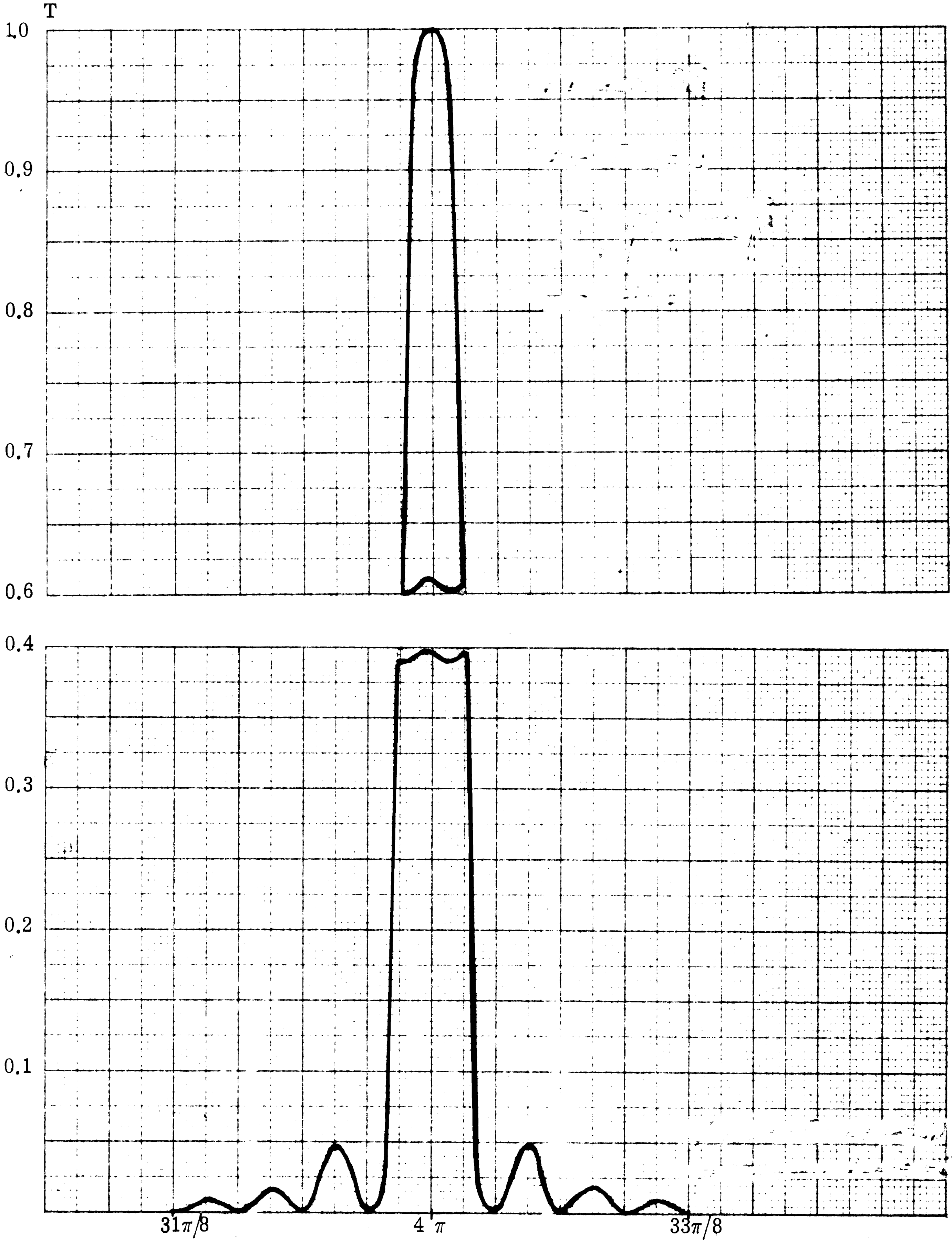

FIG. 3-9: THE FUNCTION $T = (\sin 2^N\theta / 2^N \sin\theta)^2$ FOR N=5. ANGULAR RETARDATION OF THINNEST PLATE $= 2\theta$.

in free space

$$B_f = \frac{0.5\ c}{d_N \mu} , \qquad (3.30)$$

while the normalized band width from the frequency approach produces the same result as (3.29). Note that the frequency band width for the polarization filter of a given length is independent of frequency, which is desirable in the laser communications channel.

Quartz has been one of the birefringent materials used in commercial polarization filters. The quantity μ has a value of 0.011 for quartz so that for a band width of 10^9 cps, d_N must be 13.6 meters. This is clearly too great a thickness for a practical filter, quartz plates would limit a filter to a band width of an order of magnitude or two wider than 10^9 cps. Calcite, another material that has been used for the polarization filter, has a μ value of 0.172, so d_N in this case must be 87.2 cm which is a more realistic thickness but still impractically large. A list of values of refractive indices for some birefringent materials is shown in Table V. It can be observed that the μ value for calcite is exceeded by that of only two other materials, but the difference is not enough to make the filter dimension less than 40 cm for a band width of 10^9 cps. It seems then, in light of presently available materials, that the band width requirement of 10^9 cps cannot be achieved in a practical polarization filter.

TABLE V: VALUES OF REFRACTIVE INDICES (BILLINGS[23])

Crystal	Class	Indices
ADP	Tetragonal	ϵ = 1.4792
		ω = 1.5246
KDP	Tetragonal	ϵ = 1.4684
		ω = 1.5095
Rochelle Salt	Orthorhombic	α = 1.492
		β = 1.493
		γ = 1.496
EDT	Monoclinic	α = 1.5086
		β = 1.5893
		γ = 1.5930
Quartz	Hexagonal	ϵ = 1.553
		ω = 1.544
Calcite	Hexagonal	ϵ = 1.486
		ω = 1.658
$NaNO_3$	Hexagonal	ϵ = 1.3361
		ω = 1.5874
Rutile	Tetragonal	ϵ = 2.903
		ω = 2.616
Mica	Monoclinic	α = 1.503 to 1.623
		β = 1.545 to 1.685
		γ = 1.545 to 1.704

ϵ extraordinary refractive index of uniaxial crystal

ω ordinary refractive index of uniaxial crystal

α, β, γ smallest, intermediate and largest refractive indices of biaxial crystal.

The absorption within the birefringent material of which the filter is constructed has not been considered above. The attenuation of a wave propagating through a lossy medium can be accounted for by an attenuation constant α such that

$$I(x) = I_o e^{-\alpha x} \tag{3.31}$$

where α can be a function of frequency. I(x) is the intensity at a point x within the medium measured in the direction of propagation from the reference point where the intensity is I_o. In the filter whose Nth element has a thickness $d_N = 2^{N-1} d_1$ where d_1 is the thickness of the first element, the total plate thickness is

$$d_T = \sum_{i=1}^{N} d_i = (2^N - 1) d_1 .$$

Thus, the output from the last plate of the filter is decreased from that given in (3.26) by the additional factor

$$T_\alpha = e^{-\alpha(2^N - 1) d_1} \approx e^{-\alpha 2^N d_1} , \tag{3.32}$$

since $2^N >> 1$ for $N \geq 5$. From expression (3.30), we can obtain then

$$T_\alpha = e^{-\left[\alpha c/\mu B_f\right]} . \tag{3.33}$$

The transmission is seen to decrease exponentially with decreasing bandwidth, so a further narrowing of the bandwidth is eventually achieved, depending upon the magnitude of α, only through rapid reduction of the peak transmission of the filter.

Another mechanism which decreases the peak filter transmission is the reflection occurring at the various interfaces. This can be reduced in practice by use of refractive index matching cements to join various components of the filter, or by immersing the filter in an oil whose refractive index is near that of the filter components. Reflection losses will generally be less important than absorption losses and will not be dealt with here.

As a practical example, polarization interference filters have been made commercially by Baird Associates (Greenler[25]) using quartz plates having a bandwidth of 1 Å at 6563 Å and with a peak transmission on the order of 10 %. Steel, et al[26] describe a filter using quartz and calcite plates with a bandwidth of 1/8 Å at the same wavelength, having a peak transmission of 12 %.

The aperture and field of view of the filter are also characteristics which are of interest. The field of view is determined by the maximum off-axis effects that can be tolerated in the filter. Evans[22] considers this problem in detail and and so it will not be discussed here.

3.5. Tuning of the Polarization Filter

The utility of the polarization interference filter can be greatly enhanced by devising a means for tuning it. A slight amount of tuning can be obtained by varying the temperature of the filter, since the refractive index and thus the retardation of the birefringent plate is a function of the temperature. The control which can be obtained in this manner is, however, limited to a few angstroms and may actually become a nuisance in a narrow band filter since then it must be very accurately temperature regulated.

A second method suggested by Lyot[27] for tuning the filter is the obvious one of changing the plate thickness. He proposed the scheme of making the individual plates in the form of two wedges which could be slid across each other, thus varying the length of the light path through the wedge combination. This results in the requirement for very fine adjustments to be made in synchronism to each plate of the filter and does not represent a truly variable filter.

A third and most practical method for tuning of the polarization filter is the addition of a variable achromatic phase plate or retardation plate to each fixed element so that one can vary the retardation of each section of the filter. The achromatic phase shifter, which is, by definition capable of producing a phase shift independent of the wave length, could give results exactly comparable to those obtained by the use of variable thickness plates mentioned above. The retardation plate on the other hand, one example of which that is adjustable being the Kerr cell, produces a retardation dependent on the wavelength and so does not give results as good as those obtainable with an achromatic phase shifter. Billings[24] and Evans[22] consider this problem. The discussion below follows Billings' treatment.

The tuning is accomplished by varying the retardation of each section so that its nearest transmission peak is shifted to the place where the overall filter transmission is to be a maximum. If, at the desired wave length λ_x the retardation of the Nth plate is

$$\Gamma_{Nx} = x + 2^{N-1} n_1 = 2^{N-1} \Gamma_1 \quad ,$$

the argument of the cosine is given by

$$\theta_{Nx} = \pi (x + 2^{N-1} n_1) = 2^{N-1} \theta_{1x} \quad ,$$

where n_1 is the number of waves retardation for the first plate's nearest peak. The nearest peak of the Nth plate has as the argument of its cosine

$$\theta_{Nn} = (n_N + 2^{N-1} n_1)\pi$$

where n_N an integer and is so chosen as to minimize $|n_N - x|$.
It is convenient to number the peaks of each plate starting with zero at the natural filter transmission peak.

The retardation plate is now used to shift θ_{Nx} to the value θ_{Nn} without changing the wave lengths λ_x by adding an additional retardation δ_{Nx} such that

$$2\,\theta_{Nx} + \delta_{Nx} = 2\,\theta_{Nn} \qquad (3.34)$$

Thus the transmission peak is shifted to the wave length λ_x. We can mention here that δ_{Nx} will vary with wavelength for the retardation plate, but for the achromatic phase plate it does not. The relation above can be put into another form, the utility of which will be apparent below. Thus, equivalent to (3.34)

$$\theta_{Nn} = a_N \theta_{Nx} \tag{3.35}$$

so that

$$a_N = \frac{2^{N-1} n_1 + n_N}{2^{N-1} n_1 + x} \tag{3.36}$$

When the Kth plate is considered, then ,

$$a_K = \frac{2^{N-1} n_1 + 2^{N-K} nK}{2^{N-1} n_1 + x} \tag{3.37}$$

The relation between θ_{Kx} and θ_{1x} is determined, it should be noted, only by the fact that $d_K = 2^{K-1} d_1$, so that $\theta_{Kx} = 2^{K-1}\theta_{1x}$. But now, the retardation of each filter section is given by $a_K \theta_{Kx}$ so that the 1:2:4: etc., relation between the sections of the filter is no longer true. Thus ,

$$T_x = \left[\cos a_1 \theta_{1x} \cos a_2 2\,\theta_{1x} \cos a_3 2^2 \theta_{1x} \ldots \cos a_N 2^{N-1} \theta_{1x}\right]^2, \tag{3.38}$$

so that while the peak of the filter has been shifted to wavelength λ_x, the side bands peaks may occur with different spacing and amplitudes than for the unshifted peak, where T is given by (3.26). Billings[24] points out, however, that the various a_i values may be the same for several of the filter sections, and with an n_1 value of 2 or more, there is no significant distortion in the filter characteristics or increase in residual light transmission even when the filter is tuned far from a natural peak. It is obvious that the larger the variation of the a_i's from 1, the greater will be the effect on the filter characteristic. At its largest deviation from 1, the value of a_K is

$$a_K = 1 \pm \frac{1}{2^K n_1 + 1} \quad . \tag{3.39}$$

Thus the variation is relatively small for the thicker sections, and this maximum deviation occurs when the maximum retardation, 1/2 wave, is required to be added to or subtracted from the Kth section.

The phase shift δ_{Kx} may be expressed as

$$\begin{aligned} \delta_{Kx} &= 2\left[\theta_{Kn} - \theta_{Kx}\right] \\ &= 2^K \theta_{1x} \left[a_K - 1\right] \\ &= 2\theta_{Kx} \left[a_K - 1\right] \quad , \end{aligned}$$

where, it should be recalled, θ_{1x} is 1/2 the retardation angle of section 1 at λ_x. If a_K is substituted for from (3.37) and the formula

$$x = 2^{N-1} n_1 \frac{(\lambda_o - \lambda_x)}{\lambda_x}$$

is used, where λ_o is a reference wavelength, then

$$\delta_{Kx} = \frac{\lambda_x(n_K + 2^{K-1} n_1) - 2^{K-1} n_1 \lambda_o}{n_1 \lambda_o} \; 2\pi \tag{3.40}$$

λ_o is the wave length at which the Kth section has a retardation angle of $2\theta_{Kn}$, and λ_x is the wave length at which the Kth section has a retardation angle of $2\theta_{Kx}$. Billings[24] has plotted the retardation in waves which must be added to the plates of a three element filter in order to shift its pass band continuously from $0.8\,\lambda_c$ to $1.33\,\lambda_c$, where the first plate has a retardation of 4π at λ_c.

When the achromatic phase shifter is considered, then the retardation which is added is independent of the wave length. As a result, the transmission peak of each section is merely shifted along the wavelength scale to the desired point of an overall peak without distorting the transmission characteristics of the filter even when tuned far from a natural peak. As Evans[22] points out, however, tuning by the method of shifting the nearest peak of each filter section to the desired transmission peak is a practical possibility whether the phase shifter is achromatic or not, since the results obtained with the retardation plate and achromatic phase shifter are comparable.

3.6. Comments and Conclusions

Based on the results of the preceding analysis and calculations, the prismatic or Wernicke type filter appears to be unsuited for application in a laser communication channel due to the limitation on the narrowness of the passband. In addition, the tuning of such a filter is impractical and is incompatible with the requirement of a narrow passband.

It has been shown above that the polarization interference filter is capable of producing arbitrarily narrow passbands, at least theoretically, when the absorption is ignored. However, when considered from a practical viewpoint, the thickness of material required to produce a passband of 10^9 cps is prohibitive when presently available materials are considered. Tuning of the polarization interference filter is theoretically possible over a 2:1 band using electro-optic techniques.

3.7. Future Work

Work will be continued during the next quarter on the transmissivity characteristics of other types of optical filters and the possibility of tuning them.

IV. Bibliography

1. Barasch, M. L., G. Hok, P. Lambropoulos and E. K. Miller, "Study of Problem Areas in Optical Communications," Interim Report No. 1, 06515-1-T, University of Michigan Radiation Laboratory (31 July 1964).

2. Goldberg, L., "The Absorption Spectrum of the Atmosphere," The Solar System: Vol. II-The Earth as a Planet, University of Chicago Press (1958).

3. Altshuler T. L., "Infrared Transmission and Background Radiation by Clear Atmospheres," General Electric Missile and Space Vehicle Department Document No. 615D199 (December 1961).

4. Watanabe, K., "Ultraviolet Absorption Processes in Upper Atmosphere," Advances in Geophysics-5, Academic Press, New York (1958).

5. MacDonald, J. E., "Physics of Cloud Modification," Advances in Geophysics-5 (1958)

6. Rollins, R. A., Jr and F. Zwas, "Investigation of Space Communications Using Lasers," University of Michigan Institute of Science and Technology Report 5693-9-T (May 1964).

7. Deirmendjian, D., "Scattering and Polarization Properties of Water, Clouds, and Hazes in the Visible and Infrared," Applied Optics, 3, No. 2, 187(Feb. 1964).

8. Gates, D. M. and C. C. Shaw, "Infrared Transmission of Clouds," J. Opt. Soc. Am., 50, No. 9, 876(Sept. 1960).

9. Curcio, J. A., "Evaluation of Atmospheric Aerosol Particle Size Distribution from Scattering Measurements," J. Opt. Soc. Am., 51, No. 5, 548(May 1961).

10. Kurnick, S. W., R. N. Zitter and D. B. Williams, "Attenuation of Infrared Radiation by Fogs," J. Opt. Soc. Am., 50, No. 6, 578(June 1960).

11. Elterman, L., "Parameters for Attenuation in the Atmospheric Windows for Fifteen Wavelengths," Applied Optics, 3, No. 6, 745(June 1964).

12. Gordon, J. P., "Quantum Effects in Communication Systems," Proc. IRE, 50, 1898(Sept. 1962).

13. Louisell, W. H., A. Yariv and A. E. Siegman, "Quantum Fluctuations and Noise in Parametric Processes-I," Phys. Rev., 124, 1646(1961).

14. Gordon, J. P., "Quantum Noise in Communication Channels," Conference Quantum Electronics, Paris, Vol. 1, 55(1963).

15. Feynman, R. P. and F. L. Vernon, Jr., "The Theory of a General Quantum System Interacting with a Linear Dissipative System," Annals of Physics, 24 118(1963).

16. Stern, T. E., "Information Rates in Photon Channels and Photon Amplifiers, IRE International Convention Record, Pt. 4, 182(1960).

17. Shimoda, K., H. Takahasi and C. H. Townes, "Fluctuations in the Amplification of Quanta with Applications to Maser Amplifiers, "J. Phys. Soc. Japan, 12, 685(June 1957).

18. Kruse, P. W., L. D. McLauchlin and R. B. McQuiston, Elements of Infrared Technology, John Wiley and Sons (1962).

19. Peters, C. J., "Gigacycle Bandwidth Coherent Light Traveling-Wave Phase Modulator," Proc. IEEE, 51, No. 1 (1963).

20. Lyot, B., Comptes Rendus, 197, 1593(1933).

21. Öhman, Y., Nature, 41, 291(1938).

22. Evans, J. W., "The Birefringent Filter," J. Opt. Soc. Am., 39, 229(1949).

23. Billings, B. H., S. Sage and W. Draisin, "A Narrow Passband Polarization Interference Filter for Hydrogen Alpha," Rev. Sci. Instruments, 22, 1009(1951).

24. Billings, B. H., "A Tunable Narrow-Band Optical Filter," J. Opt. Soc. Am., 37, 738(1947).

25, Greenler, R. G., "Optical Filters," Concepts of Classical Optics -Appendix O, W. H. Freeman and Co., San Francisco (1958).

26. Steel, W. H., R. N. Smartt and R. G. Giovanelli, "A 1/8 Å Birefringent Filter for Solar Research," Australian J. Phys., 14, 201(1961).

27. Lyot, B., American Astrophys. 17, Nos. 1-2 (1944).